PHYSICAL BIOLOGY OF BIOMEMBRANES AND BIOMOLECULES (PHYBIOM)

BY

MD. MOZZAMMEL HAQUE

AtoSiM in Physical, Chemical and Biological Sciences, University of Amsterdam/Ecole Normale Superieure in Lyon

Diploma Thesis in Biophysics, Carol Davila University of Medicine and Pharmacy/Hungarian Academy of Sciences

A thesis
submitted to Middlesex University in partial fulfilment of the requirements
for the degree of
PhD by Public Works

May 2018

Approved by:

Richard Bayford
Director of Biophysics, Middlesex Cancer Research Centre for Investigative Oncology, London

Hemda Garelick, Chair
Department of Natural Sciences, Middlesex University
London

Zhanzhong Shi
Department of Natural Sciences, Middlesex University
London

Declaration

I hereby declare that this research is my own, unaided work. It has not been submitted before for any other degree, part of a degree or examination at this or any other award.

Md Mozzammel Haque   Date: 02/12/2018

Safety and Ethical Issues

I declare that this research has been subject to ethical review and received ethical approval from the Ethics Committee of Scientific Research of the University of Medicine and Pharmacy "Carol Davila" (Code PO-3-F-03, No. 34).

I also declare that I have not deviated from the terms of the ethical approval issued by this committee.

Md Mozzammel Haque   Date: 09/12/2018

Abstract

To study mechanical properties of red blood cells, the combination of an AC dielectrophoretic apparatus and a single-beam optical tweezers were used. The experiments were performed with high frequency (e.g. 10 MHz) below the second turnover point between positive and negative dielectrophoresis. The electronic response of RBCs is dominated by the local interactions with the trapping beams. The elastic modulus was determined (μ = 1.80 ± 0.5 µN/m) by measuring the geometrical parameters of RBCs as a function of an applied voltage. However, the deformation of the red cell membrane was determined (Deformed gradient =0.08) from the maximum applied voltage when a spherical RBC escapes to the electrode from the trapping centre. These results were compared with similar experimental values obtained from other techniques. This is easy to use an alternative method to determine the mechanical properties of RBCs.

Solute transport across cell membranes (e.g. RBC membrane) is the ubiquitous phenomenon, whose diffusion rate depends on the narrowest portion of membrane pores and the architecture of diffusing solutes. When a solute is confined in the critical area of membrane pores, which shows a quite different behavior compared to the homogenous bulk fluid whose transport is isotropic in all directions. The solute size and shape have been determined using the allometric scaling law, which explores the variation in the diffusion coefficient for solutes of different size and structure in physiological environments. Overall rates of diffusion through cell membranes have been determined based on membrane composition, local architecture, and the extend of binding.

The functional group structures of protein folding (e.g. RBCs membrane protein) have been investigated using classical quantum biology based on infrared spectroscopy in polar groups capable of forming hydrogen bonds. The equivalence of infrared radiant energy and the bending energy of oscillating atoms along bonds is reliant on the reduced Planck constant, reduced mass and bond stiffness. The defined quantum biological equation is used to determine the deformation value changes from its equilibrium bond angle, which is estimated from the molecular

geometry, in the hydrogen-bonded section of a polypeptide chain. This approach also quantifies substrates fit into the active sites of receptors by modifying the lock and key model.

Proper protein folding determination is the minimization of free potential energy and adds order to the system. However, the hydrophobic force at protein side chains has been determined by the enthalpic effect of solutes, which may play a crucial role in protein misfolding. The "wrong" solutes are the hydrophobic dominated effect, which is the major driving force for protein misfolding. The interactions between hydrophobic solutes and protein side chains involve the rearrangement of side chains by disrupting protein backbone hydrogen bonds. The hydrophobic interaction is a thermodynamic process, which has been investigated by minimizing the potential energy that changes from enthalpy to thermal energy or vice versa as a temperature. Therefore, the enthalpic temperature due to macromolecular deformation defines the temperature limit for protein misfolding. The deformation temperature limit is the lowest possible temperature achievable with protein misfolding.

Preface

This thesis has been conducted on mechanical properties of biological membranes, biomolecular structures, protein conformation, protein misfolding and aggregation. The part of the thesis was made during the transition period when I was moving from the department of biophysics and cell biotechnology in Carol Davila University of Medicine and Pharmacy to Hungarian Academy of Sciences, so in practice, I have worked in both departments. Especially, the experimental section of the thesis was done in the department of biophysics and cell biotechnology, Carol Davila University of Medicine and Pharmacy. During the experiments, I received help on how to operate optical tweezers from Prof Dr Tudor Savopol. The simulation was the part of the thesis, for which Prof Dr Andras Der, Hungarian Academy of Sciences, was helping me a lot. I am thankful to both for allowing this flexible arrangement.

I am thankful to Professor Dr Richard Bayford for giving me the opportunity to work further in this very interesting field, particularly on protein misfolding and aggregation. Prof. R. Bayford suggests me concerning the initial draft of the thesis, delivering numerous valuable comments and advice on drafting this thesis. I also thank my unfailingly supportive wife, Cristina Maria Haque, and my child, David Haque, for their patience while I engage in the research activities of which this thesis is some of the fruit.

Contents

List of publications

This thesis consists of an overview and of the following publications, which are referred to as p^I, p^{II}, p^{III}, and p^{IV} in the text.

P^I. Haque MM, Moisescu MG, Valkai S, Der A, Savopol T (2014) Stretching of red blood cells using an electro-optics trap. Biomed Opt Express 6 (1): 118-123

P^{II}. Haque MM (2015) Elastic theory for the deformation of a spherical dielectric biological object under electro-optical trapping. RSC Adv 5: 44458-44462

P^{III}. Haque MM (2017) Diffusion coefficient in biomembrane critical pores. J Bioenerg Biomembr 49: 445

P^{IV}. Haque MM (2017) Infrared studies of deformation and docking in hydrogen-bonded molecular systems. J Biomol Struct Dyn 36: 15, 4023-4028

P^V. Maque MM, Bayford R (2019) Protein misfolding thermodynamics. J Phys Chem Lett 10(10): 2506-2507

Author's contribution

The author has played an active role in all stages of the research reported in this thesis. He has performed all the experiments and analysis, ran all the simulations, and written the manuscript for publication p^{I}. In publications p^{II}, p^{III}, p^{IV} and P^{V}, the author has planned and performed all the analysis and published these papers as a single/first author in higher impact international journals. Therefore, the author has the main responsibility for the planning, execution, and writing of publications I-V.

List of abbreviations

RBCs red blood cells

DEP dielectrophoresis

pDEP positive dielectrophoresis

nDEP negative dielectrophoresis

CM Clausius-Mossotti factor

MscL mechanosensitive channel

FPR fluorescence photobleaching recovery

FRAP fluorescence recovery after photobleaching

MRI magnetic resonance of imaging

IR infrared

DNA deoxyribonucleic acid

PLL poly-L-lysine

PGA polyglutamic acid

RO5 rule of five

MjC major complex

MnC minor complex

PROMIST protein misfolding thermodynamics

1. Introduction

Cells are fundamental to life, which consist of lipids, proteins, and carbohydrates. A very important component of cells is the membrane-bound compartments that separate the living cell from its nonliving surroundings. The membrane is compartmentalized by protein-lipid and protein-protein interactions. Due to interactions and diverse constituents (Fig. 1), the membrane structure is complex, static and dynamic phenomena take place in the crucial cellular component. In addition, the dynamics of membranes are the transverse direction across the bilayer and the lateral direction in the plane of the two-dimensional matrix. The lateral movements give rise to the fluid nature of the membrane and are very important for membrane functions (Nicolson 2014). In addition to their dynamic properties, membranes are also elastic and semipermeable those regulate material transports for stable internal balance.
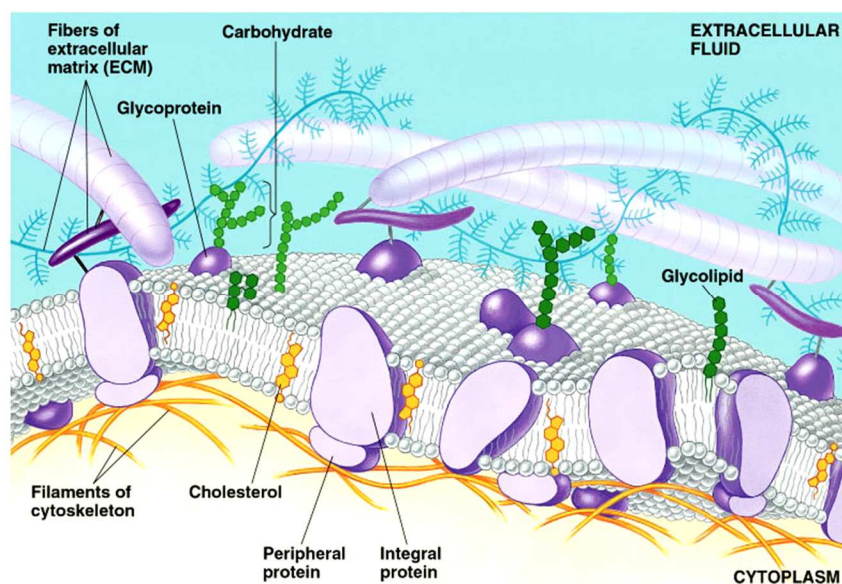
Figure 1 Schematic presentation of a cell membrane. Adapted from
https://www.thinglink.com/scene/875494412363235328

The elasticity of membranes (e.g. red blood cell membrane) is due to the membrane skeleton that is a cross-linking protein network and joints to the bilayer at some points (Kuznetsova et al. 2007) (Fig. 1). However, membrane proteins are central to cellular function and essential to cell architecture. Various types of dysfunction in membrane proteins are common causes of human diseases (Ruivo et al. 2009). Protein dysfunction causes diseases by changing the stiffness of membranes as well

as changing cell shapes (Huang and Ingber 2005; Cross 2007). The elasticity of lipid bilayers is essentially zero due to its fluidity nature; the elasticity of red blood cell (RBC) membrane is mainly contributed from the spectrin network (Li and Lykotrafitis 2014), whose experimental determined value is significantly higher than diseased cells (Haque et al. 2014, p[I]). Furthermore, RBCs are the most deformable cells, which have intrinsic mechanical properties. Measuring the deformability of the RBC surface area holds the key to understanding RBC related diseases (Silva 2011; Li 2013). The surface area expansion or compression of the RBC membrane is determined, which therefore has a constant numeric value (Haque 2015, p[II]).

The central component of the red cell membrane is a lipid bilayer, which functions as transporting hydrophobic solutes. Whereas proteins attached to or associated with the lipid bilayer are responsible for transporting hydrophilic solutes. In both cases, the rate of diffusion depends on critical pore structures, and also the size and shape of diffusing solutes (Haque 2017, p[III]). Furthermore, solutes (e.g. ions, small, large and macromolecules) can also be transported by binding with transmembrane integral membrane proteins. After transporting solutes across membranes, they can bind into sites of biomolecules, which therefore involve conformational changes, and their binding mechanism is investigated modifying the lock and key model (Haque 2017, p[IV]). However, the spatial arrangement of the receptor binding site (e.g. protein) is determined using classical quantum biology and protein misfolding is determined as the deformation temperature limit. In all papers, an extensive comparison to experiments in the case of theoretical studies is attempted.

2. Background

2.1 Physical properties of biomembranes

The structural backbone of biomembranes is lipid and protein molecules, which are formed as self-organized assemblies in the presence of water. Due to the amphiphilic nature of lipid/protein molecules in water, the hydrophobic attraction between hydrocarbon tails is their tendency to decrease their interface with water, and hydrophilic repulsion between polar heads, which incorporates a steric contribution involving the hydration layer of the polar heads. However, polar

headgroups at the surface are partially neutralized/hydrated by counter-ions/water distributed across the amphiphile-solution interface.
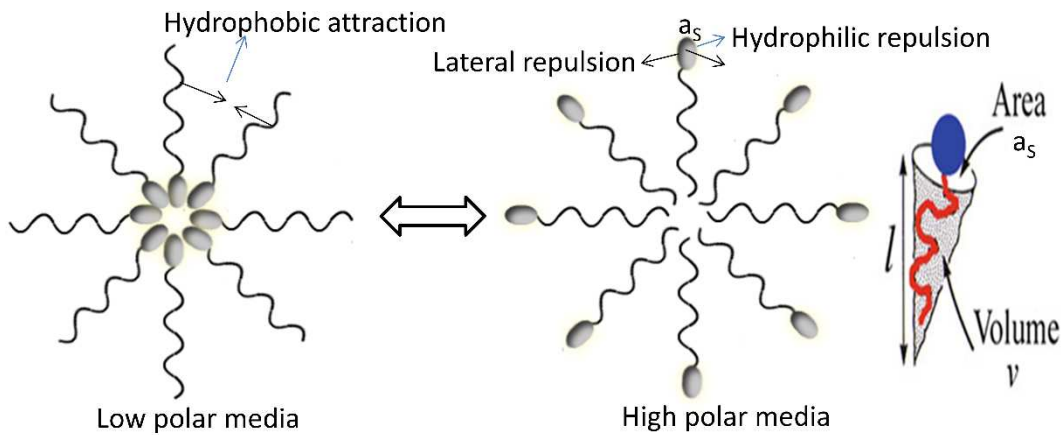

Fig. 2 Peptide/lipid micelle

The attractive and repulsive forces depend on the size of the polar headgroup, as shown in Fig. 2. If the surface area a_s of the polar headgroup increases, the repulsive force will be directly proportional to a$_s$, i.e., Γa_s where Γ is the surface tension coefficient, and the attractive force will be inversely proportional to a_s, i.e., η/a_s, where η is a proportionality constant. Mathematically, the chemical potential of the amphiphiles associated with the micelles is:

$$\mu = \Gamma a_s + \frac{\eta}{a_s}$$

In the above expression, it concludes that an increase in the area a$_s$, leads to a minimization of the repulsive component, while the attractive components minimize the chemical potential area tends to zero. For an optimum value a_0 of the polar head, μ reaches a minimum. By taking $\frac{\partial \mu}{\partial a} = 0$ gives, $\eta = \Gamma a_0^2$ and $\mu_0 = 2\,\Gamma a_0$, where μ_0 is the chemical potential for an optimum number of monomers. By substituting these expressions into μ, we obtain:

$$\mu = \mu_0 + \frac{\Gamma}{a_s}(a_s - a_0)^2$$

This equation states that the chemical potential of monomers aggregated into micelles reaches a minimum for an optimal area $a_s = a_0$ and increases for larger and smaller values of a_s (Israelachvili 1992).

13

Amphiphiles can form various different minimum energy configurations depending on the hydrophobic chain length, polar headgroup area, and the volume. The different structures have different curvatures and are arranged in accordance with the value of the packing parameter, $P = v/a_s l$. This geometrical parameters of the amphiphile to explain micellar shapes with affecting the interfacial surface area of the solvophilic headgroup a_s, the volume v, and extended length l of the aliphatic tail (Nagarajan 2002; Antonietti 2003; Jonsson et al. 2001) (Fig.2). The parameter, $v/a_s l$, controls the critical packing shape and most stable structure for a given amphiphile in a given solvent environment. For instance, large headgroup areas (e.g., ionic amphiphiles in low salt) favour conical packing shape, $v/a_s l < 1/3$, and spherical micelles. On the other hand, cylindrical packing shapes (e.g., double-chained lipids with small headgroups, $v/a_0 l_c \sim 1$) favour planar bilayer, while a truncated cone, $v/a_S l \sim \frac{1}{2}-1$, favours a vesicle. All these possible structures, the planar bilayers and vesicles are of greatest relevance to the living matter.

The effective lipid shape, as a measure of its ability to fit into a particular lipid aggregate, is very important to form and participate in a bilayer structure (Cooke and Deserno 2006). However, the effective shape is a property of lipid molecules that are influenced by the geometrical constraints imposed by the aggregate in order to maximize hydrophobic interactions among their tails and hydrophilic interactions among their heads. During the aggregation, there are three different forces (the lateral pressure profiles) that act inside the lipid bilayer for stabilization (Marsh 2007; Xing et al. 2009). These forces are the repulsive forces that act between the headgroups (Fig. 2), the interfacial tension that acts in hydrophobic/hydrophilic-hydrophilic interfaces as a result of the hydrophobic/hydrophilic effect, and the entropic repulsion between the flexible fatty-acid chains. When the lipid bilayer is in equilibrium, these forces have to sum up to zero, but the rather large interfacial tension from the two bilayer interfaces has to be distributed over a short range. The lateral pressure of the interior of the lipid bilayer has to counterbalance this interfacial tension γ, also called the line tension or interfacial energy, over a distance corresponding to the bilayer thickness d_L. Therefore, the lateral pressure density of the bilayer is the force per unit area, which becomes $2\gamma/d_L$, (Thiam et al. 2013). This lateral pressure density is used to influence the molecular conformation of proteins embedded in the lipid bilayer. For instance, the hydrophobic interaction between

proteins and lipids gives rise to interfacial tensions for hydrophobic matching during the formation of red blood cells. However, hydrophobic residues at the border between membrane lipid and channel proteins maintain the tension sensitive conformation.

The interfacial tension, which acts so as to make the interface as small as possible, imparts certain stiffness to the interface. The lateral pressure density corresponds to the interfacial stiffness, which characterizes the spherical shape of the lipid bilayer. However, the interfacial stiffness can be softened by the introduction of interfacially active molecules e.g. amphiphiles like proteins, which accumulate in the interface and lower the interfacial tension. When the interface is fully covered by proteins (e.g. red blood cells), the interfacial tension tends towards zero, where the stability and conformation of the interface are controlled by conformational entropy and by the elastomechanical properties of the interface. The elastomechanical properties of red blood cells come from the spectrin network at the interface (Stokke and Mikkelsen 2009). However, spectrin is a polymeric protein that can cross-link with other spectrin molecules into a two-dimensional network (Fig. 1). This polymer displays some rigidity at a shorter scale and also is flexible, but provides a certain shear resistance. Therefore, the red blood cells show the shear stress, in which the stress is parallel to the surface of the cell. Furthermore, the red cell membrane acts as a capacitor, because it consists of a thin dielectric situated between two ionic conductors (e.g. outer is a phosphate buffer solution and inner electrolytes-cytoplasm).

3. Elasticity of red blood cells

3.1 Functions of RBC compositions

The lipid bilayer tension is related to the force needed to deform a membrane. Due to interfacial tension at the polar-polar interface, lipid bilayers can spontaneously form closed spherical structures (e.g. vesicles, lysosome), when mixed in excess water. But in the case of red blood cells, the lipid bilayer plasma membrane is closely associated on the cytosolic side with an elastic protein network because the lipid bilayer (negative charge headgroups or zwitterionic) that has strong interaction with a protein, e.g. cytochrome c that acts as a capacitor and

serving as the dielectric (Minerick et al. 2003). The plasma membrane has no shear resistance due to its fluid nature (Li et al. 2017), while the membrane skeleton is comparatively soft, which resists both stretch and shear deformation (Pegoraro et al. 2017). In addition, the main role of the membrane skeleton is to provide elastic net, which inhibits strong local deformations of the lipid bilayer.

Bending and changing the shape of a red cell membrane involves both deformations of the fluid lipid bilayer as well as the elastic deformation of the cytoskeleton that is a tethered membrane with a certain resistance to shearing. The relationships between the stresses and the deformations of red blood cells are determined by the elastic moduli of the tethered cross-linked proteins and the lipid bilayer. The membrane skeleton is a concentrated solution of proteins such as spectrin, actin, transmembrane anchoring proteins and glycophorin. The spectrin is polymeric, constructed from units, which are tetrameric associations of two heterodimers in head-to-head association (Fig. 3).

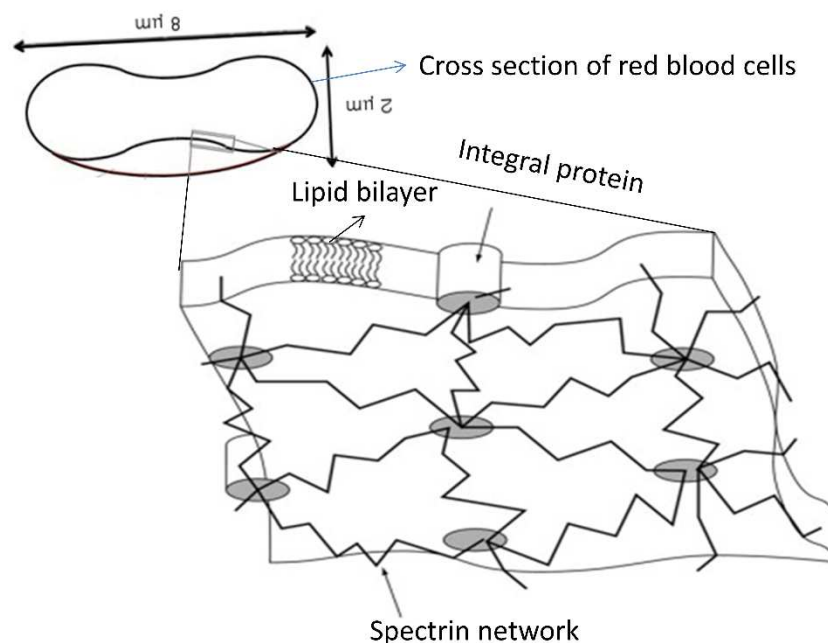Fig. 3 Typical sketches of RBC membrane
(Seen from the cytoplasmic side)

Each junction of the protein network is a protein complex, which, coupled to the lipid bilayer. Therefore, the main elastic components of the membrane skeleton are spectrin polymers determined solely by its internal structure. The lipid bilayer is locally incompressible due to its fluid-like behaviour, but has no resistance to static

shear deformations, on the other hand, the membrane skeleton resists shear because of spectrin network, but relatively easily compressible. When the membrane skeleton is compressed or expanded locally, spectrins, which anchor the skeleton, must move relative to the incompressible lipid bilayer fluid with viscous drag and consequent dissipation.

3.2 Shapes of RBCs

Generally, a healthy blood cell has a biconcave shape. When the lipids are extracted from the cell membrane, the shape of the spectrin network becomes almost spherical. Hence, the precise red blood cell shape is a manifestation of a coupling between the lipid bilayer properties and the elastic properties of the cytoskeleton. Cholesterols are predominantly incorporated in the outer leaflet of the lipid bilayer, which thus changes the physical properties as well as the shapes of erythrocyte, e.g. echinocyte, discocyte, stomatocyte etc (Meeuwissen et al. 2011; Lim et al. 2002). The medium of cell suspending solution is hypotonic, isotonic and hypertonic, which also affect the shape of the red cell. For example, if RBCs are suspended in a hypotonic solution, its shape is changed from biconcave to spherical.

3.3 Forces acting on RBCs in laser tweezers

When a blood cell is immersed in phosphate buffer solution (isotonic), there are various forces acting on the cell and these forces are shown in Fig. 4.
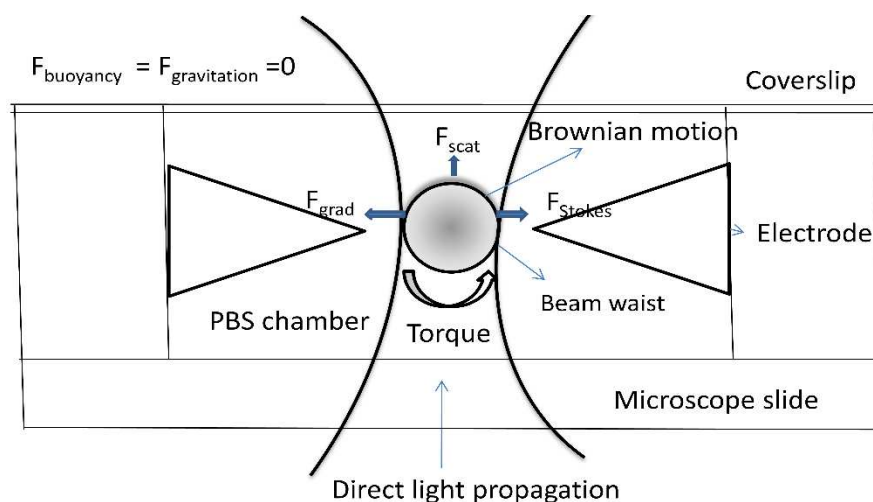

Fig. 4 Red blood cell trapping

17

The red cell can be trapped using the forces of laser radiation pressure (Lee et al. 2017). The radiation pressure is the force per unit area on a blood cell due to changes in light momentum. For stable trapping (Zhong et al. 2013), the gradient force acts transversely and the scattering force axially, and the gradient force must be larger than the scattering force. By strongly focusing a laser beam, which can create a large electric field gradient on the blood cell that acts as the radial displacement of the cell from the center of the trap. However, trapping of a spherical cell by a laser is a competition between radiation pressure (due to reflection) and gradient forces (due to refraction).
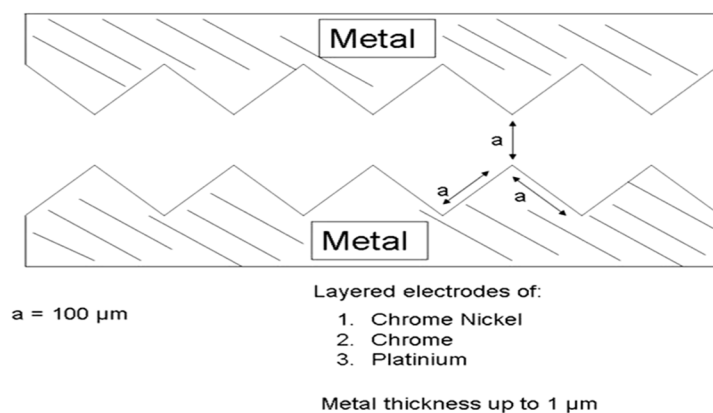

Fig. 5 Electrode geometry

For small displacements in the trapping centre where the gradient force acts as a Hooke's law force. But the cell inside of the trapping centre is not static. It vibrates and rotates in the centre of the trap (see Fig. 4). In addition, the cell in the trapped centre experiences a random force due to the thermal energy of the system, causing it to continuous motion and rotation. To overcome this Brownian motion, the cell requires very high electric field strength to exceed the thermal energy. Applying the high electric field on the cell to stretch it is the dielectrophoresis in which a force is exerted on the dielectric cell when it is subjected to a non-uniform electric field (Xue et al. 2017).

3.4 Electro-optical trap

To determine the elasticity and deformation of an RBC, the cell was suspended in a low dielectric medium (phosphate buffer isotonic solution) on the triangular electrode (Fig. 5) for positive dielectrophoresis, pDEP. At the steady-state condition,

when the cell moves under the influence of pDEP force, and this force corresponds to the drag force, and other forces (e.g. Buoyant force, Gravity) can be ignored due to the closed system, coverslip (Fig. 4). When an AC electric field was applied, the blood cell was stretched by the pDEP force via a pair of triangular electrodes (Fig. 5) from the trapped centre in a laser tweezers (Fig. 4). During performing the experiments, the voltage was gradually increased to escape the cell from the trapped centre to the electrode. The spatial distribution of the electric field between the electrodes was determined using the COMSOL Multiphysics 4.3a programming.

3.5 Stiffness of RBCs

By measuring the geometrical parameters of the stretched cell as a function of the applied voltage, the elastic modulus of RBCs was determined *(µ = 1.80 ± 0.5 µN/m)* (Haque et al. 2014, p[I]) and compared the result with similar values of the literature obtained by other techniques, such as micropipette aspiration (*6-10 µN/m*) (Hochmut 2000), dual-beam optical tweezers (Sivaramakrishnan et al. 2013) and magnetic twisting cytometry (*10-20 µN/m*) (Fedosov et al. 2010). Our experimental values are lower compared with other techniques because the lack of mechanical contact of the probe leads to adhesion and active cellular response. In addition, various forces acting upon the suspended cell were minimized while measuring the RBC stiffness.

3.6 Deformation of RBC membrane

Since the lipid bilayer is fluid/flexibility, its mechanics is dominated by its resistance to bending, which is characterized by the bending modulus. On the other hand, the elasticity of the cytoskeletal protein network is characterized by stress and shear moduli. For smooth shapes of red cells (Piety et al. 2015), the membrane skeleton is not subject to significant stress and inhomogeneity, so the shear modulus does play a very important role in shape determination. Since the red cell is the perfectly incompressible material deformed elastically at small strains and its Poisson's ratio along the axial direction is exactly 0.5 (Haque 2015, p[II]), and it is also dielectric in nature, so its deformation can be determined experimentally. During the experiments by the electro-optical trapping apparatus, the non-uniform electric field

was applied to the RBC, then the cell was escaped from the trapping centre to the electrode, which means that the trapping force of the laser tweezers is equal to the applied electrical force. Equating both the forces, the shear modulus of RBCs was calculated, of which the resulting deformed gradient is 0.08 (Haque 2015, p[II]). Therefore, this number 0.08 represents the surface deformation of the red cell. Furthermore, the deformation of cells is related to malfunctions (Lee and Lim 2007), and the number 0.08 may be used as a diagnostic parameter for underlying diseases such as diabetes mellitus, hypertension, arteriosclerosis, coronary artery disease, cancer etc.

4. Transport properties of red cell membrane

The cell membrane is the gateway for solutes (both hydrophilic and hydrophobic) that travel into and out of the cell and protects the cell from toxic elements. Hydrophobic solutes can pass through the lipid bilayer, whereas proteins embedded in the lipid bilayer are called channel proteins help to move hydrophilic solutes across the membrane (Stein 2012). In addition, transport proteins play important roles in the transmission of signals to and from nerves (Lodish et al. 2000). Whereas, lipids in the cell membrane contain lipid-soluble and water-soluble regions, a property that is basic to the role of lipids as building blocks of cell walls for transporting solutes. Membrane lipids rich in unsaturated fatty acids/shorter hydrocarbon chains are more fluid than those dominated by saturated fatty acids because the kinks in the unsaturated fatty acid tails prevent tight packing, which favours the transport process.

Cholesterol molecules are hydrophobic, short and rigid, they fill the spaces between neighboring phospholipid molecules left by the kinks in their unsaturated hydrocarbon tails (Yeagle 1985). Therefore, cholesterol tends to stiffen the bilayer, making it less permeable. However, the hydrophilic headgroups/integral proteins are hydrogen bonded with water, which exhibits the polar-polar interface due to unequal forces between water and lipid headgroups/proteins (Wilson and Pohorille 1994). These forces at interfaces favour the pore formation. In addition, this results in increased viscosity of the lipid headgroups/proteins as their rotation and mobility are constrained to stabilize pores.

To form a hydrophilic pore, the long poly-peptide integral membrane proteins are water-soluble folded proteins in a way that arranges for the hydrophobic amino acids to be inside away from water and the hydrophilic amino acids on the outside facing water (Ott and Lingappa 2002). In contrast, membrane-spanning proteins are inside-out, such that the trans-membrane part has hydrophobic amino acids facing the lipid membrane and sometimes hydrophilic or charged amino acids towards the interior. Dictated by lipids, integral membrane proteins are therefore bound to be amphiphilic i.e. hydrophobic in the middle and hydrophilic in the two ends (Cymer et al. 2015). However, for solute transport in cell membranes, proteins associated with the lipid bilayer in several different ways, which are illustrated in Fig. 5.
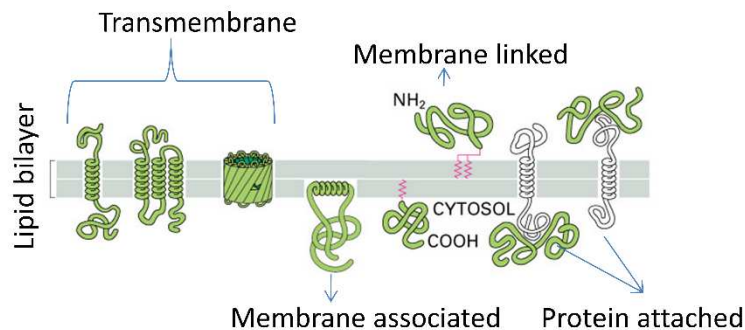

Fig. 6 Lipid bilayer embedded with proteins

On the other hand, peripheral membrane proteins anchored that are located entirely outside of the lipid bilayer, on the cytoplasmic or extracellular side, yet are associated with the surface of the membrane by noncovalent bonds (Johnson and Cornell 2002). These are usually held in place by ionic forces with the phospholipid headgroups or other proteins (Hanakam et al. 1996; Ben-Tal et al. 1997; Sankaram and Marsh 1993). Lipid-anchored proteins are outside the layer of the membrane but are covalently attached to lipids, which are within the membrane (Silvius 2003; Baumann and Mennon 2002). These peripheral membrane proteins are enhanced and stabilized the hydrophilic pores.

5. Theoretical background of membrane pore

There are two types of pores formed in cell membranes, one of which is hydrophobic for transporting hydrophobic solutes, and the other of which is hydrophilic to hydrophilic solutes. A hydrophilic cylindrical/toroidal pore/vesicle may

form by the lateral repulsion between hydrated polar lipid headgroups of lipid molecules and integral membrane proteins. But the spontaneous cylindrical pore formation of lipid hydrocarbon chains is very unlikely, which has shown detail in publication p[III]. During the self-assembly of lipids in water, the interfacial tension γ formed in the water-lipid interface is balanced by the headgroup lateral repulsion and also by the lateral repulsions between the hydrocarbon chains (Fig. 2). On the other hand, the surface tension Γ at a water-lipid interface is very low, so other factors, such as bending rigidity and spontaneous curvature C_0 play an important role in the free energy determination. However, adding the curvature energy to the energy of membrane tension, the total energy bending of area $\ss$ with a curvature C is

$$F_{Bending} = \Gamma\ss + \frac{1}{2}\kappa\ss(C - C_0)$$

Where κ is the bending rigidity of the membrane. Since the curvature is constant everywhere on the sphere, so integrating over the whole membrane yields

$$F_{Sphere} = \frac{\kappa}{2}\left(\frac{2}{R}\right)^2 4\pi R^2 = 8\pi\kappa, \text{ where } C = \frac{1}{R}$$

Therefore, the free energy of a spherical membrane is

$$F_{Sphere} = \Gamma\ss + 8\pi\kappa$$

This result is very instructive for several reasons. First, from this equation, it is concluded that the membrane free energy is independent of the sphere size, but depends on the surface area. For κ = *10-20 K_BT* (Fang et al. 2017), the free energy to form vesicles/pores is in the range 250-500 K_BT. However, this is the large energy penalty to make vesicles/pores (Fig. 6), and this intrinsic energy cost can be overcome is by incorporating proteins that favour the curved state (Simunovic and Voth 2015).

Insertion of membrane proteins into lipid bilayer creates tensions due to the unequal forces at the protein-lipid interface (Diz-Munoz et al. 2013; Pontes et al. 2017). Besides tensions, the dipole moments of the lipid polar headgroups and water act the formation of the pore (Jordan et al. 1989).
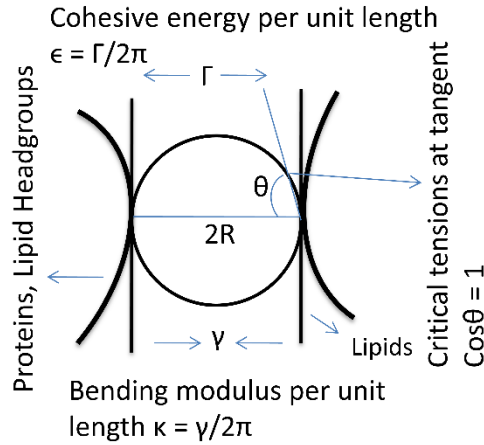
Fig. 7 Membrane pore/vesicle

The surface tension Γ is the force exerted by the membrane per unit length of the circumference of the pore (Fig. 7). The infinitesimal force acting on an infinitesimal arc dc of the circumference is given by

$$\Gamma dc = \Gamma R d\theta$$

Where R is the generic radius of the pore. $d\theta$ is the infinitesimal angle subtended by the arc dc. The infinitesimal work done by Γ is given by

$$\Gamma dc = \Gamma R d\theta dR$$

Therefore, the work of formation of a pore of radius R is given by

$$\Delta F_\Gamma = \int_{R=0}^{R} \int_{\theta=0}^{2\pi} \Gamma R d\theta dR = \Gamma \int_{R=0}^{R} R dR \int_{\theta=0}^{2\pi} d\theta = \Gamma \pi R^2$$

In the case of thermodynamics, the membrane represents the closed system, whereas the rest of the universe that interacts with the system is referred to as the surroundings. The surface tension works to increase the pore size, which is directed out toward the pore rim, whereas the surroundings are directed toward the centre of the pore. Both forces exactly counterbalance each other in the case of thermodynamically reversible processes. Since the surroundings work opposite to the displacement, so the resulting work done by the surroundings on the systems will be negative. Therefore, this can be written as the following equation:

$$\Delta F_{sd,\Gamma} = -\pi R^2 \Gamma$$

23

In addition to this work, the line tension γ acts tangentially at a generic point of the pore rim (Fig. 7). Therefore, the work done by the line tension is given by

$$\Delta F_\gamma = - \int_{C=0}^{2\pi R} \gamma dc = -2\pi R\gamma$$

Since the line tension tends to contract the rim length, so during the expansion of the pore, the work done by the line tension will be negative due to its direction is opposite to that of the displacement. However, the pore expansion is thermodynamically reversible; the work done by the surroundings is counterbalanced by the line tension. Thus, the work done by the surroundings can be written as:

$$\Delta F_{sd,\gamma} = 2\pi R\gamma$$

However, the overall mechanical work is the pore-free energy change done by the line and surface tension at the polar-polar/apolar interface. Therefore, pore-free energy can be written as:

$$\Delta F_{Pore} = 2\pi\gamma R - \pi R^2\Gamma$$

In addition to the mechanical work, an electrical work ΔF_{elc} is also involved in the membrane pore formation due to the dipole moment of water (Disalvo et al. 2004; Kanduc et at. 2014; Shimanouchi et al. 2011; Langner and Kubica 1999). Since water has higher polarizability than lipid molecules and membrane proteins, so they can be replaced by water molecules. Hence, such a replacement is favoured by the application of a transmembrane potential $\Delta\Psi$ and contributes to the enlargement of the pore radius R (Disalvo 2015; Yang et al. 2008; Tielrooij 2009). In other words, the progressive insertion of water molecules along the periphery of the pore moves the periphery outward, which amounts to a positive work done by the membrane system. Consequently, the surroundings must accomplish a negative work of equal magnitude to generate a pore under thermodynamically reversible conditions. For the pore filled with water molecules, the work done by the system is equal in magnitude but opposite in sign to the electrical work done by the surroundings. Therefore, the total reversible work spent by the surroundings will be of the following simplified form:

$$\Delta F_{sd,elc} = 2\pi R\gamma - \pi R^2\Gamma - \pi R^2 (\frac{1}{2}\Delta\Phi\Delta\Psi^2)$$

Where $\Delta\Phi$ is the difference in capacitance per unit surface area. $\Delta F_{sd,elc}$ implies that the formation of a hydrated membrane pore not only depends on the mechanical work but also the transmembrane potential $\Delta\Psi$. When at $\Delta\Psi=0$, $\Delta F_{sd,elc}$ is essentially equal to the mechanical work ΔF_{pore}. Since the transmembrane potential depends on the dipole-dipole interactions, so an increasing electrostatic interaction tends to decrease the pore radius by making a negative contribution to the free energy of pore formation. But at equilibrium, where there is no electrostatic interaction, the mechanical work for the pore formation is $\Delta F_{pore}=\pi\gamma^2/\Gamma$ at the critical radius of $R^*=\gamma/\Gamma$, which therefore is the energy barrier for the pore formation. The pores with the radius below the critical value are reversible and tend to close, whereas the "supercritical" ones grow unlimitedly, eventually causing membrane breakdown. Therefore, outside of the critical radius, there is no internal structure of pore formation from an originally intact bilayer. The critical pore/core radius depends on the mechanical forces, which are found in the all domains of life, where the mechanical forces work on polar-polar/non-polar interfaces as a response to the line and surface tensions in the membrane. Based on the membrane composition and the minimization of interfacial free energy, the critical pore structures for different pores are determined, which are shown in Table 1.

Table 1 shows the critical radius of the membrane pores.

Pores/Cores	Line tension (γ)	Surface tension (Γ)	Critical pores/cores (R^*)
Cylindrical pore	Γ	Γ	$R^* = \dfrac{\gamma}{\Gamma}$
Toroidal pore	Γ	Γ	$R^* = \dfrac{\gamma}{\Gamma}$
Hydrophilic pore	Γ	Γ	$R^* = \dfrac{\gamma}{\Gamma}$
Hydrophilic carrier pore	$\gamma = 2\pi\kappa_B$	$\Gamma = 2\pi\epsilon$	$R^* = \dfrac{(-)m\widetilde{\kappa_G}}{\kappa_B c_0}$
Porin cylindrical pore	Γ	Γ	$R^* = \delta = \dfrac{\gamma}{\Gamma}$
Lipid vesicle/Liposome/Ionophore pore	$\gamma = 2\pi\kappa_B$	$\Gamma = 2\pi\epsilon$	$R^* = \dfrac{\kappa_b}{\epsilon} = \dfrac{1}{2}\sqrt{S^*}$

Where, m= slope, $\widetilde{\kappa_G}$ = Gaussian bending modulus, κ_B= bending modulus, c_0 = spontaneous curvature, S^*= Critical surface area, ϵ= Cohesive free energy

6. Tensions at bending interfaces

Pores lined with hydrophobic tails are hydrophobic pores and if they are lined with lipid polar headgroups/proteins are hydrophilic pores. Lipids with relatively large charged headgroups in water (such as lysophosphatidylcholine, lysolecithin, or lysophosphatidic acid (Kooijman et al, 2005)) promote positive lipid monolayer curvature because of higher interfacial energy at the water-lipid headgroups/protein interface. While lipids with relatively small headgroups in water (such as PE or cardiolipin) promote negative lipid monolayer curvature due to the higher repulsion between water and lipid hydrocarbon chains compared to headgroups-water interfacial energy. On the other hand, uncharged lipids with longer acyl chains and smaller headgroups would be less likely to form the curved structure. Both types of curved monolayer lipids together promote the formation of lipid pores/liposomes due to the bilayer asymmetry achieved by generating a difference in the lipid compositions of the two monolayers (Stillwell 2013; Marquardt et al. 2015; Eeman and Deleu 2009; Zalba and ten Hagen 2017). In addition, more lipid/cholesterol/protein molecules can be incorporated into the outer raft monolayer than the inner monolayer of a stable bending (Galimzyanov et al. 2016). Protein insertion into the bilayer is not only generating membrane asymmetry but also creates interfaces such as polar-polar and polar-apolar (Jarsch et al. 2016; Phillips et al. 2009; Kozlov 2010; Derganc et al. 2013; Scott 2017; Gilbert et al. 2014). In principle, the interfaces (e.g. protein-water, protein-lipid etc.) are in higher energy states than the rest of the membrane. This gives rise to a property known as line tension, analogous to surface tension associated with interfaces. The line tension constricts patch boundaries, whereas the surface tension constricts the surface area of interfaces (Ben M'barek et al. 2017). Both tensions, which here are referred to as $\prod_{member}$, at interfaces work together to increase or decrease the pore radius R formed in the membrane (Harmandaris and Deserno 2006). Since the lipid bilayer can be represented by a two-dimensional mathematical surface, so the surface tension at polar-polar/apolar bending interface is the angular cohesive free energy $\epsilon = \Gamma/2\pi$, which depends on the membrane composition. The membrane composition characterizes by the bending modulus κ that is higher than the symmetric membrane (Elani et al. 2015), which can be determined by the following relation:

$$\kappa = \frac{1}{2\pi} \Pi_{membr} \, R_{pore}$$

In the above expression, the bending modulus is directly proportional to the tensions and the radius of the membrane pore. The line tension works along the pore edge for stabilizing the membrane (Kuzmin et al. 2005), whereas the surface tension stabilizes a pore. In order to minimize the line tension, the membrane pore tends to be a circular shape, while the surface tension works the membrane pore maintain a smaller size. For a stable membrane pore, both tensions work together as counterbalancing each other for minimizing the free energy (Pannuzzo and Bockmann 2014). In addition, the line tension works at the edge of membrane domains or at the lipid phase separations, phospholipid height mismatch and steric interactions (Garcia-Saez 2007; Noguchi 2012), so it can be determined by the bending modulus of the membrane. However, this term depends on the internal membrane properties, such as its elastic parameters and the chemical structure of membrane-forming different lipids (Molotkovsky and Akimov 2009; Akimov et al. 2014; Panov et al. 2014. For a given domain size, the line energy is the smallest when the interface is smallest, meaning that the domains to be circular with a radius $R = \frac{1}{2} \sqrt{S}$, where S is the domain area. In this case, the free energy formed by the line tension will decrease due to membrane domain formations. On the other hand, the surface tension corresponds to work on the lateral tension tends to be closed in the pore (Akimov 2017). However, the work performed by the lateral tension to open a pore depends on membrane bending, cohesion, and adhesion (Akimov et al. 2017). Thus, the net free energy will be an angular surface tension of the membrane bending including cohesion and adhesion for a pore (Haque 2017, p[III]).

7. Membrane pore formation

7.1 Hydrophobic mismatches

Membrane proteins have hydrophobic regions (usually a hydrophobic α-hairpin formed by two α-helices) inserted within the lipid membranes (Huang and Huang 2017; von Heijne 2006; Shukla et al. 2015; Zurek et al. 2011; Bogdanov et al. 2014; Killian 1998).
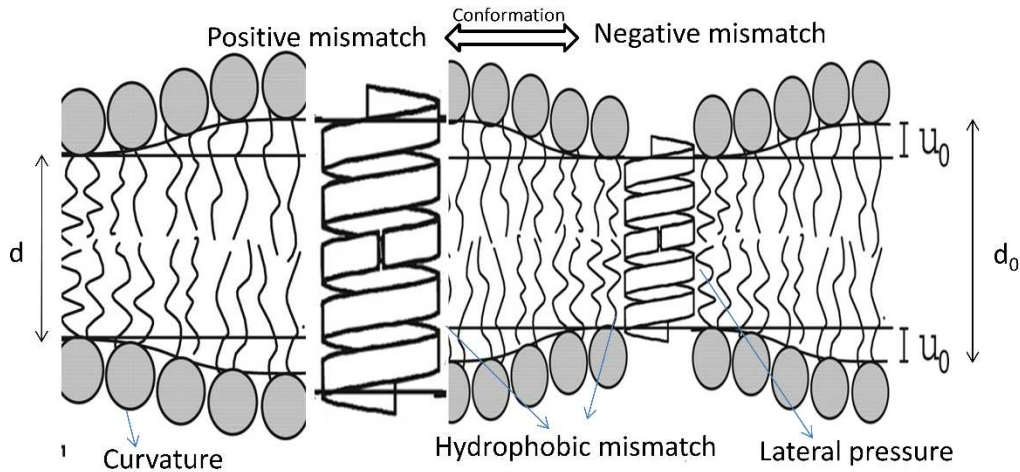
Fig. 8 Hydrophobic mismatches

The β-helixes, on the other hand, are soluble proteins, with a small hydrophobic content, which therefore need to join forces (oligomerize) in order to form a hydrophobic surface large enough to insert in the lipid bilayer (Shatursky et al. 1999; Cosentino et al. 2016). The difference between the thickness of hydrophobic regions of a transmembrane α-hairpin/ oligomer and of the lipid membrane it spans is the hydrophobic mismatch.

7.2 α-hairpin insertion in lipid bilayer

During the insertion, a mismatch in thickness between the hydrophobic core of the protein and that of the lipid bilayer has an associated energy cost, which can be calculated as the following mismatch free energy (Fig. 8) (Milovanovic et al. 2015; Lundbaek et al. 2009; Ramadurai et al. 2010),

$$\Delta G_{mismatch} = \frac{1}{2} k_{eff} u_0^2 c, \text{ Where } u_0 = \frac{1}{2}(d_0 - d)$$

Where κ_{eff} is the effective bending modulus. This hydrophobic mismatch energy induces membrane and/or protein deformation (Jesus and Allen 2012). The membrane deformation free energy is expressed as a quadratic function of the spring constant associated with the extent of membrane deformation $u_0 = \frac{1}{2}(d_0-d)$, (Fig. 8), where d_0 and d represent the hydrophobic thickness of the unperturbed and local membrane, respectively (Andersen and Koeppe 2007; Saric and Cacciuto 2013). The mismatch of interactions at the coexistence of two different hydrophobic

regions leads to the so-called line tension-the two-dimensional equivalents of surface tension. In addition, the presence of a hydrophobic mismatch in membranes can promote transmembrane domain tilt by changing the conformation of proteins, and oligomerization (Park and Opella 2005). These effects will be more pronounced in the presence of the aromatic and heterocyclic residues such as tryptophan, tyrosine, and histidine because of these hydrophobic nature. Furthermore, lipids with one or more carbon-carbon double bonds have more tilt angles because each double bond produces a kink in the acyl chain, creating extra free space within the bilayer, disrupting its regular packing and imparting additional flexibility to the hydrocarbon tails (Bigay and Antonny 2012; Casalegno et al. 2015; Nugent and Jones 2013; Kim et al. 2012; Wilman et al. 2014; Larson et al. 2016). Pores in membranes, therefore, are formed by tilt angles and stabilized these by the mismatch free energy (Ulmschneider et al. 2006). In addition, electrostatic interactions between lipid membranes and proteins can also affect the insertion of proteins in a lipid membrane. Usually, the main effect of an attractive electrostatic interaction between a protein and a lipid membrane is to increase the local concentration of the protein just above the membrane surface (Mulgrew-Nesbitt et al. 2006; Seeling 2004). However, the strong electric potential gradient close to the charged membrane might help orient proteins in order to promote correct insertion.

7.3 β-barrel insertion in lipid bilayer

When considering β-barrel outer membrane proteins for insertion into the hydrophobic bulk of the lipid bilayer, the length of the hydrophobic patch of the β-barrel proteins and the lipid bilayer is not always perfectly overlapping because of heterocyclic residues and unsaturated acyl chains (Tamm et al. 2004; Xu et al. 2008; Lee 2003; Slusky 2017). This difference defines the so-called hydrophobic mismatch, i.e. the difference in the length between the hydrophobic core of the lipid bilayer and the hydrophobic tertiary domain of the protein (Fig. 8). However, this hydrophobic mismatch involves an energy cost, which is called here the hydrophobic mismatch free energy cost (Marsh 2008).
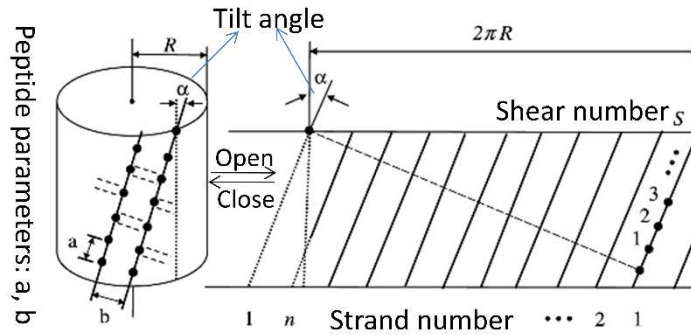
Fig. 9 Porin cylindrical pore

This mismatch free energy can be used to bring the edges of a beta sheet together to form a cylinder (Fig. 9). When the two edges come together to form a line, where a line tension is created in which its energy cost determined is $2\pi R\gamma$. However, for a stable cylindrical pore, shear is created by sliding the two edges parallel to that line, and the energy cost of the sliding will, therefore, be $\pi R^2 \Gamma$. Here, in both cases, the cylindrical pore radius is R, which depends on the tilt angle α (or shear number S) and the number of β-strands n. The tilt angle or the shear number is the displacement (Liu 1998), which is determined as the ratio between the line tension to the surface tension (Haque 2017, p[III]).

7.4 Conformational change of carrier proteins

When solutes bind with integral membrane proteins for transport across membranes, the conformations of membrane proteins are changed (Fig. 10). The energy utilized to change conformations come from the binding energy.
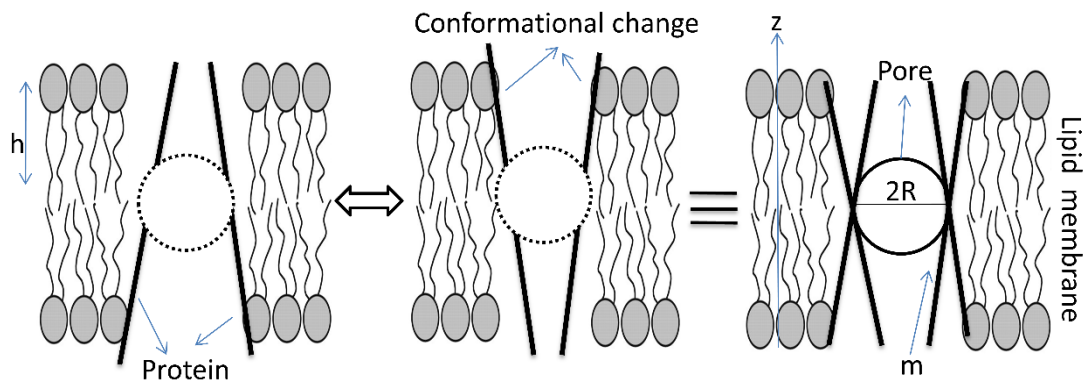

Fig. 10 Carrier membrane pore

Using the lateral pressure profiles, the difference in free energy between the two conformational states of the protein (non-tilted and tilted states) modelled as a truncated cone (with radius R and slope m) can be calculated (Fig. 10). For this calculation, the radius of the cone in the centre of the bilayer is kept constant and the radius as a function of the normal coordinate z is then written as $r\,(z) = R + mz$, where m is the slope of the cone. Thus, one can write the favourable free energy difference for the conformational change of proteins:

$$\Delta G_{\text{conformation}} = \int_{-h}^{h} dz p(z)\left[\pi R^2 - \pi(R + mz)\right] = -2\pi Rm(\kappa_b c_0) - \pi m^2 \kappa_G$$

Where z is the normal coordinate of the layer, h is the thickness of the monolayer, κ_b is the bending modulus, κ_G is the Gaussian bending modulus, and c_0 is the spontaneous curvature.
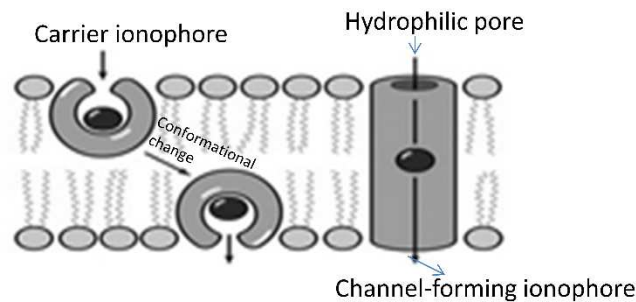

Fig. 11 Ionophore pore

In the case of transporting ions across lipid membranes as ion carriers (Fig. 11), the electrostatic forces during the binding that stabilized the complex are no longer greater than the unfavourable free energy change of cyclisation and the ionophore releases its enclosed cation and reverts to the low energy acyclic conformation (Azzaz 2015; McNaught and Wilkinson 1997). This conformational change in the ionophore delivers the ion to the interior of the cell due to the lipid-soluble ionophore exterior, a cage like interior that is capable of binding and shielding ions (Fig. 11) (Antonenko and Yaguzhinsky 1988; Alfonso and Quesada 2013). Ion-binding selectivity is, therefore, the balance of non-covalent effects such as ion-ionophore, solvent-ionophore, ion-solvent and solvent-solvent interactions (Anchaliya and Sharma 2017). Furthermore, the ion selectivity is dependent on the ionic size, which can fit in the pore cavity formed by the lipid membrane/polyether/protein (Wang et al.

2001) in the lipid bilayer membrane, for example, gramicidin dimerizes and folds as a right-hand β-helix (David and Rajasekaran 2015; Benincasa at al. 2015), and the dimer spans the bilayer to form a cylindrical pore (Fig 11). The hydrophobic outer surface of gramicidin dimer interacts with the core of the lipid bilayer while the ions pass through the more polar lumen of the helix. Gating (open/close) of gramicidin channels is thought to involve reversible dimerization. The cavity/pore diameter of an ionophore can be calculated based on the selectivity of cation complexation according to its radius. A conformational change in the gramicidin during complexation to solute is an alternative method to determine the cavity diameter, see Table 1 (Haque 2017, p[III]).

7.5 Protein conformation and aggregation

A conformational change, which is a change in the shape of a macromolecule, plays an essential role in the biological function of proteins. The shape change of proteins is generally induced by many factors such as temperature, pH, voltage, ion concentration, phosphorylation and the ligand binding. The binding process may not only involve changes in internal energy or entropy but can also involve changes in molecular shapes. Folding and unfolding are crucial ways of regulating biological activity and targeting proteins to different cellular locations, and also have a tendency to form aggregates, as summarized in Fig. 12. Protein folding/misfolding in water is the hydrophobic effect, which arises from the fact that water molecules on a hydrophobic surface seek to form hydrogen bonds with each other or with other polar molecules (Rocha et al 2004). The folding process always involves a change in a multitude of random-coil conformations to a single folded protein structure, in which it decreases in randomness and thus a decrease in conformational entropy (Baruah et al 2015; Tzeng and Kalodimos 2012), $-\Delta S_{Conf}$ and an overall positive contribution to free energy ΔG. However, folding of a globular protein is a thermodynamically favored process, i.e. the free energy ΔG_{therm} must be negative and minimized:

$$\Delta G_{therm} = \Delta H - T\Delta S_{conf}$$

Where T is the absolute temperature. ΔG_{therm} changes from positive to negative or vice versa, where $T=\Delta H/\Delta S_{Conf}$. A negative ΔG_{therm} is a result of features that yield a large negative enthalpy ΔH or any other increase in entropy on folding.

Metal ions can play a role as modulators of protein conformations. When a globular protein has lost all of its non-covalent bonds by the interaction with transition metals, it becomes unfolded. In the unfolded state (Fig. 12C), the intramolecular hydrogen bond between proteins is broken and formed protein-to-water hydrogen bonds due to the presence of metal ions (pH drop ~ 4.4-6), and this, in turn, increases the entropy of the solvent (Liu et al 2000; Pabon and Amzel 2012). In addition, the presence of metal ions in the solvent not only breaks the non-covalent bonds but also destabilizes the hydrophobic part of proteins (Mercus 2012). When the size of a metal ion is comparable to that of a water molecule, the hydrogen bonding network of the surrounding water does become significantly affected. While small and multiple charged ions with higher charge density have a stronger interaction with hydrogen bonds and can destabilize the protein conformations.
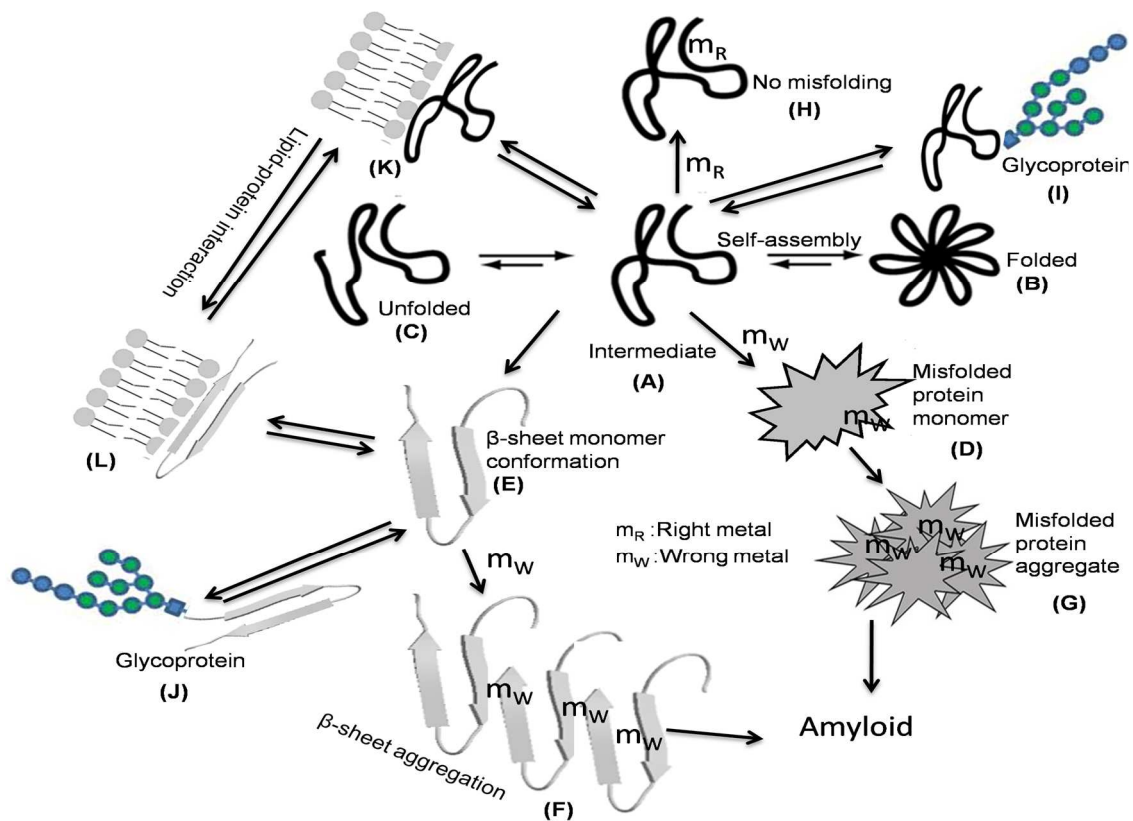

Fig. 12 Schematic of the proposed folding and aggregation pathways for amyloid formation.

In principle, the intermediate unstable states (Fig. 12A,E) between folded (native) and unfolded states control protein functions. However, the intermediate states originate from interactions between regions of the folding polypeptide chains that are separated in the native chain. These non-native states, which expose buried hydrophobic regions in the native state, are prone to self-association and subsequent aggregation with metalloproteins (wrong metals) into disordered complexes (Fig. 12D,F,G) because wrong metals are the hydrophobic dominated effect in an aqueous solution. In addition, wrong metals enhance electrostatic interactions in protein-protein complex formations, which are essential in protein aggregation (Miravalle et al. 2000; Massi and Straub 2001; Chiti et al 2003). Consequently, metalloproteins (Fig. 12G,F), glycoproteins (Fig. 12I,J), and protein-lipid complexes (Fig. 12K,L) promote misfolding and aggregation due to the increasing hydrophobic effect and the surface-immobilized metal ions. On the other hand, water on protein active site surfaces behaves differently from bulk water, which is categorized as either kosmotropes (polar water structure makers) or chaotropes (water structure breakers). Since metal-protein non-covalent bonds are stronger than water-protein bonds (kosmotropes and chaotropes), so immobilized metal ions/protein surface free radicals may enhance misfolding and aggregation of proteins (Tsumoto et al 200).

8. Biomolecular deformation

8.1 Molecular recognition

During the conformational changes of the integral membrane protein, biological complexes, which involve specific recognition by receptors of their cognate substrates, are among the most characteristic processes of living organisms (Amaral et al. 2017). The recognition between receptors and their corresponding substrates is often highly specific. The strength of binding between a receptor Ω and its corresponding substrate ζ can be described by the following simple relation:

$$\Omega + \zeta \rightleftarrows \Omega\zeta$$
$$K_{eq} = \frac{[\Omega\zeta]}{[\Omega][\zeta]}$$

Where $\Omega\zeta$ stands for the receptor-substrate complex. K_{eq} is the equilibrium binding constant. Alternatively, it is also possible to measure the binding affinity in terms of inhibition constant K_i, which is $K_{eq}= 1/K_i$ or by an IC_{50}-value, which is the concentration of an inhibitor that is required to displace 50% of the specific binding of the labelled substrate. The selective binding of a substrate to a receptor is determined by the structural and energetic recognition of a substrate and a receptor. The binding affinity, which corresponds to a Gibbs free energy of binding, can be determined from the experimentally measured binding constant:

$$\Delta G = -\check{R}T\ln K_{eq} = \Delta H - T\Delta S, \text{ Where } \check{R} = \text{Ideal gas constant}, T = \text{Temperature}$$

This relation implies that macromolecular recognition is associated with a decrease in entropy ΔS (due to a decrease in disorder); however, the recognition takes place spontaneously due to free energy ΔG minimization. The non-bonded interaction between the substrate and its receptor can be estimated based on the free energy change, which in turn is the sum of the free energy change due to electrostatic, hydrophobic, inductive, and stacking interactions. The entropy decreases between water and its receptor are also compensated by the removal of water from the interacting surface.

8.2 Bending vibrations

The binding site of the receptor is a functional group, which possesses a unique spatial arrangement for each functional group (Zhou 2010). The spatial arrangements or positioning of atoms or a group of atoms around an asymmetry binding centre can determine the shape of a functional group, which is known as the molecular geometry. However, the spatial arrangements are unique for each functional group, which can determine from the molecular geometrical shape. In principle, the bonding atoms of a functional group are not static, they are dynamic (Fig. 13). Their bending vibrations will decrease if they are hydrogen-bonded. Recognition of the hydrogen-bonded functional group by the substrate is driven by energetic. The total free energy comes from the binding between the substrate and its receptor is equal to the energy of bending motion plus hydrogen-bonded fluid

viscosity. Furthermore, binding of a substrate to a receptor can induce an atomic motion in the receptor that leads to the change of the shape of that receptor.
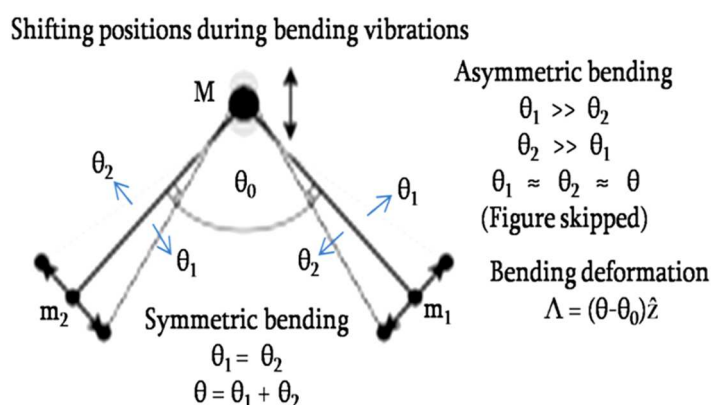

Fig. 13 Bending vibrations

This shape change by bending vibrations makes a chemically important cavity inaccessible to other molecules, which is called the selectivity of the substrate. However, the motion is associated with kinetic and potential energies of bending motion. The maximum bending potential energy stores in bonds and the potential energy of bonds including hydrogen bonds are being converted to the kinetic energy of the bending spring, and vice versa.

8.3 Bending equation of motion

The bending motion is the lateral motion of the reduced mass as a function of time is governed by a linear second order ordinary differential equation with constant coefficients. Therefore, the bending equation of motion can be written as the following:

$$\mu \frac{d^2 \Lambda}{dt^2} = -\kappa \Lambda$$

Where μ is the reduced mass of the three-atom system (Haque 2017, p[IV]) (Fig. 13). The overall "κ" parameter controls the stiffness of the bonds' bending spring (Haque 2017, p[IV]) (Fig. 13). Λ defines the angular displacement during the motion from its equilibrium angle θ_0. The solution to this equation of simple harmonic oscillator is

$$\Lambda(t) = A\cos(\omega t); \ \omega = \sqrt{\frac{\kappa}{\mu}}$$

This equation implies that the motion is periodic, repeating itself in a sinusoidal fashion with constant amplitude A. When the two bonds are bent, they store elastic potential energy, which in turn is transformed into kinetic energy. However, the potential energy depends on the bonds' stiffness including hydrogen bonds and the reduced mass of oscillating atoms. In the case of hydrogen-bonded systems, the overall stiffness of bonds increases (Cantrell 2015; Shahbazi 2015; Baruah and Khan 2013; Li et al. 2011), which, in turn, decreases the bending motion, as shown in Fig. 14. In addition, hydrogen bonding increases the bending restoring force and also the viscous force (Briscoe et al. 2000; Christensen et al. 2015; Sulzner and Luft 1997). During the complex formation, the active functional group of a substrate imposes a strain on the bonds in the transition state through electrophilic and nucleophilic forces, but the strain energy is lower than the bond breaking or the dissociation energy due to bending vibration.
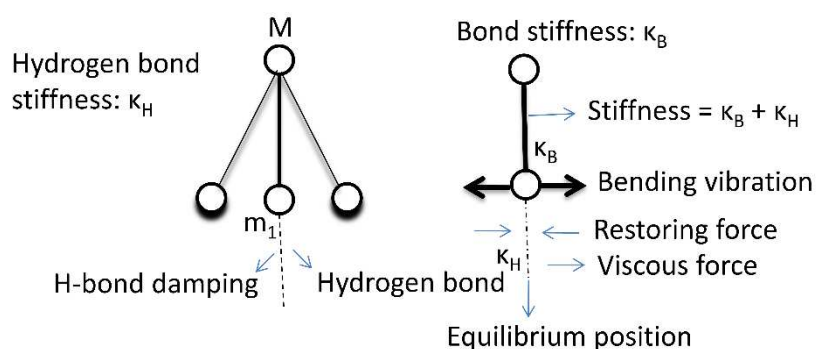

Fig. 14 Hydrogen bonded bending vibrations

Since the bending spring acts as lateral vibrations, so the damping effect on restoring and viscous forces can be cancelled out. Therefore, the net force is the force of bending spring in correlated three-atomic systems, which is determined using the parallelogram law (Haque 2017, p[IV]) (Fig. 13). After all, it is called a simple harmonic oscillator, and it undergoes simple harmonic motion: sinusoidal oscillations about the equilibrium bond angle, with constant amplitude and a constant angular natural frequency.

8.4 Molecular conformations using infrared

When the natural vibrational frequency of bonds in the three-atomic systems matches the frequency of the infrared, then absorption occurs. Absorption utilizes the interaction of an applied electromagnetic field with the phonon bending vibrational field of the molecule to provide structural information. If the energy of the bending vibration corresponds to the infrared region of the electromagnetic spectrum with the matter, then molecular vibrations will be infrared active, which is illustrated below.
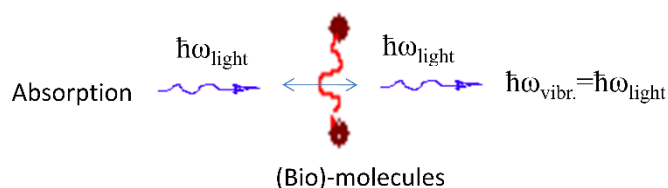
(Bio)-molecules

According to quantum mechanics, the energy of molecular bending vibration is quantized, meaning that the bending vibrational frequency will remain the same for all molecules, only the amplitude will change. Since energy is conserved, so the energy is directly proportional to the amplitude squared. The equation below describes this energy change looks like Hooke's law, which involves a bond angle.

$$\Delta_{Bending} = \frac{1}{2}\kappa(\theta - \theta_0)^2 = \frac{1}{2}\kappa\Lambda^2$$

Where $\Lambda = (\theta - \theta_0)$ defines the angular displacement/deformation (Fig. 13). The force required to bend the spring is the derivative of the energy with respect to the bending motion is the energy gradient. However, the infrared region of the electromagnetic spectrum contains natural angular frequency corresponding to the energy of bending motion.

$$\hbar\omega = \frac{1}{2}\kappa\Lambda^2 = \hbar\sqrt{\frac{\kappa}{\mu}}$$

$$\Lambda = \pm\sqrt{2}\hbar\left(\frac{1}{\mu\kappa}\right)^{\frac{1}{4}}$$

From the above equation, it is concluded that when passing infrared through molecules, the bond angle deformation Λ during bending motion in a functional group of molecules is independent of frequency.

The derived quantum biological equation Λ is used to determine the deformation value changes from its equilibrium bond angle θ_0, which is estimated from the molecular geometry in the hydrogen-bonded section of a polymer chain (Haque 2017, p[IV]). The deformation active site of a receptor can be determined by Λ, which has a unique geometric shape for each functional group. This allows the substrate to fit perfectly and changes to its working conformation due to hydrogen bonds and van der Waals forces (Hatzakis 2014; Csermely et al. 2010). In addition, the active site deformation indicates a continuous change in the conformation and shape of a receptor in response to substrate binding (Keskin 2007; Kim et al. 2013). However, the reactive group on the receptor active site is optimally positioned to interact with the substrate (Du et al. 2016). This forms a transitional intermediate, which lowers the activation free energy and allows the substrates to proceed towards the number of products at a faster rate.

9. Molecular topology: orientation & connectivity

The change in shape is crucial to protein function and control. Alteration of the protein structure by a physical process, which is driven by hydrophobic force, changes the shape and function of the protein. Due to the absence of amino acid sequence, DNA and RNA, protein misfolding depend on the molecular topology, which controls the shape of a molecule through deformation of functional and hydrophobic groups. During the complex formation, the substrate is set in motion by modifying the receptor-substrate interaction (Sauvage et al 2010). The deformation occurs through the interactions by covalent, non-covalent and non-bonding interactions between receptor and substrate active sites. Not only interactions but also conjugation of π-electron and/or lone pair in active sites may change shape (Fig. 2). In principle, the deformation is the theory of shapes, which are allowed to stretch, compress, flex and bend, not to bond breaking, but without tearing, glueing, and keeping the constant molecular weight (Barin et al 2012). For instance, let us consider open polygonal chains with the angle-fixed functional groups at each point, which are called fixed angle chains. In the case of lone pair/anion conjugation, fixing the angle is the opposite extreme of allowing universal motion, which thus distortions in both angle and length, as illustrated in Fig. 15. The overall shape of a substrate is the connectivity of folds and domains based on numbers of secondary structures

(Mashaghi et al. 2014). The substrate folding is concerned with the spatial properties/angular asymmetry of the functional groups that are preserved under continuous deformations during the interaction with the receptor. This is because substrate geometrical features become blurred due to vibrations and Heisenberg relation.
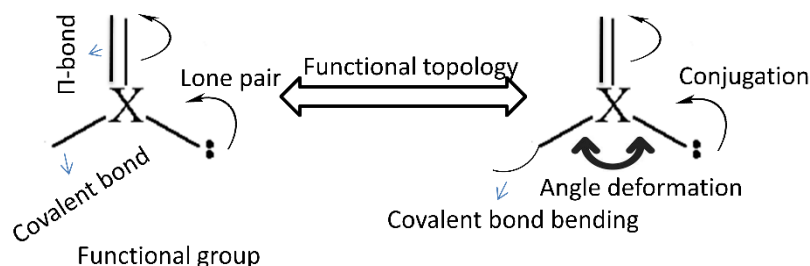

Fig. 15 Molecular topology

The changing of geometric features is the concept of topological chirality, which represents the formed gradient factor in the functional configuration space (Bruns and Stoddart 2016) (Fig. 15). At all levels, the substrate chirality is a function of the gradient vector. As the gradient vector used for the substrate deformation has the deformation temperature, this sets the limit to the temperature of deformation between the system enthalpy/van't Hoff enthalpy ΔH (Huddler and Zartler 2017) and the thermal energy $\kappa_B T_{Deformation}$ (Kinetic and potential energy). This defines the deformation temperature limit, which is

$$T_{Deformation} = \frac{\Delta H}{K_B \tau}$$

At equilibrium, $\kappa_B T_{Deformation}$ and ΔH are equal (Left side of Fig. 15), which sets a limit on the amount by which the protein can be misfolded (Right side of Fig. 15). As the protein misfolding transition has the shape-changing, this sets the limit to the temperature of the protein after deformation, $T_{Deformation}$. This is usually much higher than the absolute temperature, which is the deformation temperature associated with the interaction during the formation/aggregation of the receptor-substrate complex. When an interaction effect is present, there is no change of molecular weight ω and the size δ, but the shape τ is changeable, whose relation can be written in the following form (Haque 2017, p^{IV}):

$$\delta_{min} \propto \sqrt[3]{(\upsilon\omega)} = \tau\sqrt[3]{(\upsilon\omega)}$$

In the above expression, the proportionality constant depends on the molecular topology because biological molecules do not have a precisely defined geometry. In this case, the gradient of the energy folding surface acts as a formal force within the configuration space for changing shapes. Therefore, the change of topological shape corresponds to the change in angle and length (Breitzman (2018).

10. Summary and conclusions

There are a number of experimental data published in the literature for the elastic properties of healthy red blood cells. We present an independent technique, a combination of a single beam optical tweezers and an AC dielectrophoretic apparatus, and the results are consistent with the smaller values for the elasticity of RBCs compared with other techniques. The lower values of erythrocyte membrane elasticity *(μ = 1.80 ± 0.5 μN/m*) were observed because of the lack of mechanical contact with the cells and the nonlinear dependence of the shear modulus on the mechanical stress.

The shear modulus measured in our experiments should be distinguished from the membrane area expansion modulus. Clinical evidence shows that there is a connection between erythrocyte deformability and disease. However, this connection is not fully understood. Experimental measurements of the RBC membrane surface deformed area are very difficult to carry out due to its micro-size, flexibility and fluidity. However, during the experiments, the spherical RBCs are escaped to the electrode from the tapping centre at the maximum applied voltage. Based on escaping velocity of RBCs, the membrane deformation gradient is determined to be 0.08. The insight gained about the membrane deformation can be used to make predictions on types of diseases.

The main results of solute transport across cell membranes are, in principle, experimentally testable. However, in practice, predicting the rate of diffusion is very difficult due to variability in the properties of solutes. Therapeutic agents, for example, have a multitude of sizes and shapes and, hence, their diffusion coefficients vary in ways that are not easily predictable accurately by experiments because of limitations of frequency based experiments. To minimize the experimental limitations, the architecture of diffusing solutes is determined using the

allometric scaling law. However, the critical pore structures are determined using mechanical forces at polar-polar/non-polar interfaces in cell membranes. The diffusion coefficient determined in membrane critical pores may be useful in interpreting a variety of biological phenomena such as properties of endogenous chemicals or drugs in physiological situations. Cellular physiology is quite complex, but the effective diffusion coefficient determined here may be useful for overcoming experimental difficulties with providing novel insights into diffusing solutes across membranes.

Proteins in cells are not only membrane functions for transporting solutes but also involved in different human diseases caused by misfolding and aggregation. To determine these functions, infrared spectroscopy that has the potential to become a powerful frequency-based experimental tool for investigating biomolecular topology and internal motions. Knowledge of internal motions for the preferred orientation of functional groups may be helpful to predict the protein conformation and binding affinity. Characterization of the spatial arrangement of functional groups for appropriate receptor binding sites can be used to elucidate fundamental biochemical processes such as protein folding, misfolding and aggregation. To investigate the possible molecular conformation, the proposed method is based on infrared light that is emitted or absorbed by molecules, which is therefore independent of frequency. Therefore, this method overcomes problems occurring in frequency based experiments for investigating molecular functions.

In addition, the hydrophobic effect of "wrong" solutes disrupt the non-covalent bonds (e.g. hydrogen bond, van der Waals attractions, ionic attractions) as well as destabilizes the hydrophobic core in proteins, and as a result, proteins can 'misfold'. To identify the structure the regions that are mainly involved in the transient misfolding, the deformation temperature limit is proposed by changing their conformation from protein folding to misfolding. Thus, these techniques suggest a new direction for determining biological structures, which are also expected to be an easy-to-use a simple approach to investigate the physiological properties of molecules in biological systems.

References

Antonietti N, Forster S (2003) Vesicles and liposomes: a self-assembly principle beyond lipids. Adv Mater 15 (16): 1323-1333

Andersen OS, Koeppe RE (2007) Bilayer thickness and membrane protein function: an energetic perspective. Annu Rev Biophys Biomol Struct 36:107-130

Akimov SA, Mukovozov AA, Voronina GF, Chizmadzhev YA, Batishchev OV (2014) Line tension and structure of through pore edge in the lipid bilayer. Biol Membrane 31 (5): 323-330

Akimov SA, Volynsky PE, Galimzyanov TR, Kuzmin PI, Pavlov KV, Batishchev OV (2017) Pore formation in lipid membrane II: energy landscape under external stress. Sci Rep 7: 12509

Amaral M, Kokh DB, Bomke J, Wegener A, Buchstaller HP, Eggenweiler HP, Matias P,Sirrenberg C, Wade RC, Frech M (2017) Protein conformational flexibility modulates kinetics and thermodynamics of drug binding. Nat Commun 8: 2276

Azzaz HH, Murad HA, Morsy TA (2015) Utility of ionophores for ruminant animals: a review. Asian Journal of Animal Sciences 9 (6): 254-265

Antonenko YN, Yaguzhinsky LS (1988) The ion selectivity of nonelectrogenic ionophores measured on a bilayer lipid membrane: nigericin, nonensin, A23187 and lasalocid A. Biochim Biophys Acta 938 (2): 125-130

Alfonso I, Quesada R (2013) Biological activity of synthetic ionophores: ion transporters as perspective drugs. Chem Sci 4: 3009-3019

Anchaliya D, Sharma U (2017) Selective bulk liquid membrane carrier facilitated transport of Mg^{2+} over Li^+, Na^+, K^+ and Ca^{2+} metal ions using naphthaquinone derived redox-switchable ionophores. Main Group Met Chem 40 (1-2): 27-33

Briscoe B, Luckham P, Zhu S (2000) The effects of hydrogen bonding of aqueous poly (vinyl alcohol) solutions. Polymer 41 (10): 3851-3860

Baruah PK, Khan S (2013) Self-complementary quadruple hydrogen bonding motifs: from,design to function. RSC Adv 3 (44): 21202-21217

Barin G, Forgan RS, Stoddart JF (2012) Mechanostereochemistry and the mechanical bond. Proc Royal Soc A 468: 2489-2880

Breitzman T, Dayal K (2018) Bond-level deformation gradients and energy averaging in peridynamics. J Mech Phys Solids 110: 192-204

Baumann NA, Mennon AK (2002) Lipid modifications of proteins. In DE vance and

JE vance (Eds) Biochemistry of lipids, lipoproteins and membranes (4th ed). Elsevier Science. pp37-54.

Bruns CJ, Stoddart JF (2016) The Nature of the Mechanical Bond: From Molecules to Machines. John Wiley & Sons, Inc., Hoboken

Ben-Tal N, Honig B, Miller C, McLaughlin S (1997) Electrostatic binding of proteins to membranes. Theoretical prediction and experimental results with charybdotoxin and phospholipid vesicles. Biophys J 17 (4): 1717-1727

Bigay J, Antonny B (2012) Curvature, lipid packing, and electrostatics of membrane organelles: defining cellular territories in determining specificity. Dev Cell 23(5): 886-895

Bogdanov M, Dowhan W, Vitrac H (2014) Lipids and topological rules governing membrane protein assembly. Biochim Biophys Acta 1843 (8): 1475-1488

Benincasa M, Francescon M, Fregonese M, Gennaro R, Pengo P, Rossi P, Scrimin P, Tecilla P (2015) Helical peptide-polyamine and-polyether conjugates as synthetic ionophores. Bioorg Med Chem 23 (23): 7386-7393

Ben M'barek K, Ajjaji D, Chorlay A, Vanni S, Foret L, Thiam AR (2017) ER membrane phospholipids and surface tension control cellular lipid droplet formation. Dev Cell 41 (6): 591-604, e7

Cross SE, Jin Y-S, Rao J, Gimzewski (2007) Nanomechanical analysis of cells from cancer patients. Nat Nanotechnol 2: 780-783

Cooke IR, Deserno M (2006) Coupling between lipid shape and membrane curvature. Biophys J 19 (2): 487-495

Cantrell JH (2015) Hydrogen bonds, interfacial stiffness moduli, and the interlaminar shear strength of carbon fiber-epoxy matrix composites. AIP Adv 5:037125

Christensen G, Younes H, Hong H, Smith P (2015) Effects of solvent hydrogen bonding, viscosity, and polarity on the dispersion and alignment of nanofluids containing Fe_2O_3 nanoparticles. J Appl Phys 118:214302

Csermely P, Palotai R, Nussinov R (2010) Induced fit, conformational selection and independent dynamic segments: an extended view of binding events. Trends Biochem Sci 35 (10): 539-546

Cymer F, von Heijne G, White SH (2015) Mechanisms of integral membrane protein insertion and folding. J Mol Biol 427 (5): 999-1022

Cosentino K, Ros U, Garcia-Saez AJ (2016) Assembling the puzzle: oligomerization of α-pore forming proteins in membranes. Biochim Biophys Acta 1858 (3): 457-466

Casalegno M, Raos G, Sello G (2015) Hydrophobic aggregation and collective absorption of dioxin into lipid membranes: insights from atomistic simulations. Phys Chem Chem Phys 17: 2344-2348

Du X, Li Y, Xia YL, Ai SM, Liang J, Sang P, Ji XL, Liu SQ (2016) Insights into protein-ligand interactions: mechanisms, models and methods. Int J Mol Sci 17(2): E144

Diz-Munoz A, Fletcher DA, Weiner OD (2013) Use the force: membrane tension as an organizer of cell shape and motility. Trends Cell Biol 23 (2): 47-53

Disalvo EA, Lairion F, Martini F, Almaleck H, Diaz S, Gordillo G (2004) Water in biological membranes at interfaces: does it play a functional role? An Asoc Quim Argent 92:4-6

Disalvo EA (2015) Membrane hydration: the role of water in the structure and function of biological membranes. Springer Int., Switzerland

Derganc J, Antonny B, Copic A (2013) Membrane bending: the power of protein imbalance.Trends Biochem Sci 38 (11): 576-584

David JM, Rajasekaran AK (2015) Gramicidin A: a new mission for an old antibiotic. J Kidney Cancer VHL 2 (1): 15-24

Elani Y, Purushothaman S, Booth PJ, Seddon JM, Brooks NJ, Law RV, Ces O (2015) Measurements of the effect of membrane asymmetry on the mechanical properties of lipid bilayers. Chem Commun 51: 6976-6979

Eeman M, Deleu M (2009) From biological membranes to biomimetic model membranes.Biotechnol Agron Soc Environ 14 (4): 719-736

Fedosov DA, Caswell B, Karniadakis GE (2010) A multiscale red blood cell model with accurate mechanics, rheology and dynamics. Biophys J 98 (10): 2215-2225

Fang C, Hui TH, Wei X, Shao X, Lin Y (2017) A combined experimental and theoretical investigation on cellular blabbing. Sci Rep 7: 16666

Garcia-Saez AJ, Chiantia S, Schwille P (2007) Effect of line tension on the lateral organization of lipid membranes. J Biol Chem 282: 33537-33544

Galimzyanov TR, Kuzmin PI, Pohl P, Akimov SA (2016) Elastic deformations of bolalipid membranes. Soft Matter 12: 2357-2364

Gilbert RJC, Serra MD, Froelich CJ, Wallace MI, Anderluh G (2014) Membrane pore formation at protein-water interfaces. Trends Biochem Sci 39 (11): 510-516

Huang S, Ingber DE (2005) Cell tension, matrix mechanics, and cancer development. Cancer Cell 8 (3): 175-176

Hochmuth RM (2000) Micropipette aspiration of living cells. J Biomech 33 5(1): 15-22

Harmandaris VA, Deserno M (2006) A novel method for measuring the bending rigidity of model lipid membranes by simulating tethers. J Chem Phys 125:204905

Hatzakis NS (2014) Single molecule insights on conformational selection and induced fit mechanism. Biophys Chem 186: 46-54

Hanakam F, Gerisch G, Lotz S, Alt T, Seeling A (1996) Binding of hisactophilin I and II to lipid membranes is controlled by a pH-dependent myristoyl-hsitidine switch. Biochemistry 35 (34): 11036-11044

Huang C-Y, Huang AHC (2017) Unique motifs and length of hairpin in oleosin target the cytosolic side of endoplasmic reticulum and budding lipid droplet. Plant Physiol 174: 2248-2260

Huddler D, Zartler E R (2017) Applied Biophysics for Drug Discovery. John Wiley Sons, Inc., Chichester, West Sussex

Israelachvili J (1992) Intermolecular and surface forces. 2nd ed., Academic, London

Jesus AJD, Allen TW (2013) The determinants of hydrophobic mismatch response for transmembrane helices. Biochim Biophys Acta 1828 (2): 851-863

Jonsson B, Lindman B, Holmberg K, Kronberg B (2001) Surfactants and polymers in aqueous solution. Wiley, Chichester, England

Johnson J, Cornell R (2002) Amphitropic proteins: regulation by reversible membrane interactions (review). Mol Membr Biol 16 (3): 217-235

Jordan CA, Neumann E, Sowers AE (1989) Electroporation and electrofusion in cell biology. Springer US, New York

Jarsch IK, Daste F, Gallop JL (2016) Membrane curvature in cell biology: an integration of molecular mechanisms. J Cell Biol 214 (4): 375-387

Kuznetsova TG, Starodubtseva MN, Yogeronkov NI, Chizhik SA, Zhdanov RI (2007) Atomic force microscopy probing for cell elasticity. Micron 38 (8): 824-833

Kooijman EE, Chupin V, Fuller NL, Kozlov MM, de Kruijff B, Burger KN, Rand PR (2005) Spontaneous curvature of phospholipidic acid and lysophosphatidic acid. Biochemistry 44: 2097-2102

Keskin O (2007) Binding indunced conformational changes of proteins correlate with their intrinsic fluctuations: a case study of antibodies. BMC Struct Biol 7: 31

Kim E, Lee S, Jeon A, Choi MN, Lee H-S, Hohng S, Kim H-S (2013) A single-

molecule dissection of ligand binding to a protein with intrinsic dynamics. Nat Chem Biol 9: 313-318

Kanduc M, Schlaich A, Schneck E, Netz RR (2014) Hydration repulsion between membranes and polar surfaces: simulation approaches versus continuum theories. Adv Colloid Interface Sci 208: 142-152

Kim C, Ye F, Hu X, Ginsberg MH (2012) Talin activates integrins by altering the topology of the β-transmembrane domain. J Cell Biol 197 (5): 605-611

Kozlov MM (2010) Biophysics: joint effort bends membrane. Nature 463: 439-440

Kuzmin PI, Akimov SA, Chizmadzhev YA, Zimmerberg J, Cohen FS (2005) Line tension and interaction energies of membrane rafts calculated from lipid splay and tilt. Biophys J 88 (2): 1120-1133

Killian JA (1998) Hydrophobic mismatch between proteins and lipids in membranes. Biochemi Biophys Acta 1376 (3): 401-416

Li H, Lykotrafitis G (2014) Erythrocyte membrane model with explicit description of the lipid bilayer and the spectrin network. Biophys J 107 (3): 642-653

Li X, Vlahovska PM, Karniadakis GE (2013) Continuum- and particle-based modelling of shapes and dynamics of red blood cells in health and disease. Soft Matter 9: 28-37

Lim HWG, Wortis M, Mukhopadhyay (2002) Stomatocyte-discocyte-echinocyte sequence of the human red blood cell: evidence for the bilayer-couple hypothesis from membrane mechanics. Proc Natl Acad Sci USA 99(26): 16766-16769

Lundbaek JA, Collingwood SA, Igolfsson HA, Kapoor R, Andersen OS (2009) Lipid bilayer regulation of membrane protein function: gramicidin channels as molecular force probes. J R Soc Interface 7: 373-395

Lee K, Wagner C, Priezzhev AV (2017) Assessment of the "cross-bridge"-induced interaction of the red blood cells by oprical trapping combined with microfluidics. J Biomed Opt 22 (9): 091516

Li X, Li H, Chang H-Y, Lykotrafitis G, Karniadakis E (2017) Computational biomechanics of human red blood cells in hematological disorders. J Biomech Eng 139 (2): 021008

Lee GYH, Lim CT (2007) Biomechanics approaches to human diseases. Trends Biotechnol 25 (3): 111-118

Liu WM (1998) Shear number of protein β-barrels: definition, refinements and statistics. J Mol. Biol 275: 541-545

Li D, Ji B, Hwang K-C, Huang Y (2011) Strength of hydrogen bond network takes crucial roles in the dissociation process of inhibitors from the HIV-1 protease binding pocket. PLOS One 6 (4): e19268

Liu D, Shao Y, Chen G, Tse-Dinh Y-C, Piccirilli JA, Weizmann Y (2017) Synthesizing topological structures containing RNA. Nat Commun 8: 14936

Li L-L, Qiao S-L, Liu W-J, Ma Y, Wan D, Pan J, Wang H (2017) Intracellular contribution of topology-controlled polypeptide nanostructures with diverse biological functions. Nat Commun 8: 1276

Lodish H, Berk A, Zipursky SL, Matsudaira P, Baltimore D, Darnell J (2000) Molecular Cell Biology (4th Ed). W H Freeman, New York

Langner M, Kubica K (1999) The electrostatics of lipid surfaces. Chem Phys Lipids 101(1): 3-35

Larson R, Arndt ER, Loh AP (2016) Inducing a helical kink in a model peptide antibiotic reduces peptide-membrane interaction favourability in vesicles. Biophys J 110 (3): p422a

Lee AG (2003) Lipid-protein interactions in biological membranes: a structural perspective. Biochim Biophys Acta 1612 (1): 1-40

Liu L, Yang C, Guo Q (2000) Enthalpy-entropy conpensation in protein unfolding. Chin Sci Bull 45: 1476

Slusky JSG (2017) Outer membrane protein design. Curr Opin Struct Biol 45: 45-52

Marsh D(2007) Lateral pressure profile, spontaneous curvature frustration, and the incorporation and conformation of proteins in membranes. Biophys J 93 (11): 3884-3899

Meeuwissen SA, Kim KT, Chen Y, Pochan DJ, Hest JCMV (2011) Controlled shape transformation of polymersone stomatocyte. Angew Chem Int Ed Engl 50 (31): 7070-7073

Minerick AR, Zhou R, Takhistov, Chang H-C (2003) Manipulation and characterization of red blood cells with altering current fields in microdevices. Electrophoresis 24 (21): 3703-3717

Milovanovic D, Honigmann A, Koike S, Gotfert F, Pahler G, Junius M, Mullar F, Diederichsen U, Janshoff A, Grubmuller H, Risselada HJ, Eggeling C, Hell SW, Bogaart GVD, Jahn R (2015) Hydrophobic mismatch sorts SNARE proteins into distinct membrane domains. Nat Commun 6:5984

Molotkovsky RJ, Akimov SA (2009) Calculation of line tension in various models of lipid bilayer pore. Biol Membrany 26: 149–158

Mashaghi A, van Wijk RJ, Tans SJ (2014) Circuit topology of proteins and nucleic acids.Structure 22 (9): 1227-1237

Marquardt D, Geier B, Pabst G (2015) Asymmetric lipid membranes: towards more realistic model systems. Membranes (Basel) 5 (2): 180-196

Marsh D (2008) Energetics of hydrophobic matching in lipid-protein interactions. Biophys J 94 (10): 3996-4013

Mulgrew-Nesbitt A, Diraviyam K, Wang J, Singh S, Murray P, Li Z, Rogers L, Mirkovic N, Murray D (2006) The role of electrostatics in protein-membrane interactions. Biochim Biophys Acta 1761 (8): 812-826

McNaught AD, Wilkinson A (1997) IUPAC Compendium of chemical technology (2nd ed). Blackwell Scientific Publications, Oxford

Marcus Y (2012) Ions in water and biological implications: from chaos to cosmos. Springer, Dordrecht

Nicolson GL (2014) The fluid-mosaic model of membrane structure: still relevant to understanding the structure, function and dynamics of biological membranes after more than 40 years. Biochim Biophys Acta 1838 (6): 1451-1466

Nagarajan R (2002) Molecular packing parameter and surfactant self-assembly: the neglected role of the surfactant tail. Langmuir 18 (1): 31-38

Noguchi H (2012) Line tension of branching junctions of bilayer membrane. Soft Matter 8:3146-3153

Nugent T, Jones DT (2013) Membrane protein orientation and refinement using a knowledge-based statistical potential. BMC Bioinform 14: 276

Ott CM, Lingappa VR (2002) Integral membrane protein biosynthesis: why topology is hard to predict. J Cell Sci 115: 2003-2009

Pegoraro AF, Janmey P, Weitz DA (2017) Mechanical properties of the cytoskeleton and cells. Cold Spring Harb Perspect Biol 9 (12): 1-12

Piety NZ, Reinhart WH, Pourreau PH, Abidi R, Shevkoplyas SS (2015) Shape matters: the effect of red blood cell shape on perfusion of an artificial microvascular network. Transfusion 56 (4): 844-851

Panov PV, Akimov SA, Batishchev OV (2014) Isoprenoid lipid chains increase membrane resistance to pore formation. Biol Membrany 31: 331–335

Pontes B, Monzo P, Gauthier NC (2017) Membrane tension: a challenging but universal physical parameter in cell biology. Semin Cell Dev Biol 71: 30-41

Phillips R, Ursell T, Wiggins P, Sens P (2009) Emerging roles for lipids in shaping

membrane-protein function. Nature 459: 379-385

Pannuzzo M, Bockmann R (2014) Energetic view on membrane pore formation. Biophys J 106 (1): 1-2

Park SH, Opella SJ (2005) Tilt angle of a trans-membrane helix is determined by hydrophobic mistach. J Mol Biol 350 (2): 310-318

Pabon G, Amzel LM (2012) Unfolding ubiquitin by force: water mediated H-bond destabilization. Univ Sci 17 (3): 273-281

Ruivo R, Anne C, Sagne C, Gasnier B (2009) Molecular and cellular basis of lysosomal transmembrane protein dysfunction. Biochim Biophys Acta 1793 (4): 636-649

Ramadurai S, Holt A, Schafer LV, Krasnikov VV, Rijkers DTS, Marrink SJ, Killian JA, Poolman B (2010) Influence of hydrophobic mismatch and amino acid composition on the lateral diffusion of transmembrane peptides. Biophys J 99 (5): 1447-1454

Rocha LFO, Tarrago Pinto ME, Caliri A (2004) The water factor in protein-folding problem. Braz J Phys 34 (1): 1678-4448

Silva MD, Dao M, Han J, Lim C-T, Suresh S (2011) Shape and biomechanical characteristics of human red blood cells in health disease. MRS Bulletin 35 (5): 382-388

Stokke BT, Mikkelsen A, Elgsaetern (2009) Spectrin, human erythrocyte shapes, and mechanochemical properties. Biophys J 49 (1): 319-327

Sivaramakrishnan S, Sung JM, Dunn AR, Spudich JA (2013) Dual beam optical tweezers. Encyclopedia of Biophysics, pp522-526

Shahbazi Z (2015) Mechanical model of hydrogen bonds in protein molecules. American Journal of Mechanical Engineering 3 (2): 47-54

Sulzner U, Luft G (1997) Effect of hydrogen bonding on the viscosity of alcohols at high pressures. Int J Thermophys 18 (6): 1355-1367

Sauvage J-P, Collin J-P, Durot S, Frey J, Heitz V, Sour A, Tock C (2010) From chemical topology to molecular machines. C R Chim 13 (3): 315-328

Stein WD (2012) The movement of molecules across cell membranes. Academic Press Inc London

Silvius JR (2003) Lipidated peptides as tools for understanding of membrane interactions of lipid-modified proteins. In current topics in membranes (52). Academic Press, pp 371-395

Sankaram MB, Marsh D (1993) Protein-lipid interactions with peripheral membrane proteins. In: Protein-lipid interactions (Ed. A. Watts). Elsevier, pp 127-162

Simunovic M, Voth GA (2015) Membrane tension controls the assembly of curvature –generating proteins. Nat Commun 6: 7219

Shimanouchi T, Sasaki M, Hiroiwa A, Yoshimoto N, Miyagawa K, Umakoshi H, Kuboi R (2011) Relationship between the mobility of phosphocholine headgroups of liposomes and the hydrophobicity at the membrane interface: a characterization with spectroscopic measurements. Colloid Surf B 88 (1): 221-230

Stillwell W (2013) An introduction to biological membranes: from bilayer to rafts. 1e. Academic press. Elsevier 367p

Scott H (2017) Membrane lipid asymmetry, a key property of the mammalian plasma membrane, alters the insertion of the pHLIP peptide. Biophys J 112 (3): p527a

Shatursky O, Heuck AP, Shepard LA, Rossjohn J, Parker MW, Johnson AE, Tweten RK (1999) The mechanism of membrane insertion for a cholesterol-dependent cytolysin. Cell 99 (3): 293-299

Shukla A, Dey D, Banerjee K, Nain A, Banerjee M (2015) The C-terminal region of the non-structural protein 2B from hepatitis A virus demonstrates lipid-specific viroporin-like activity. Sci Rep 5: 15884

Saric A, Cacciuto A (2013) Self-assembly of nanoparticles adsorbed on fluid and elastic membranes. Soft Matter 9: 6677-6695

Seeling J (2004) Thermodynamics of lipid-peptide interactions. Biochim Biophys Acta 1666 (1-2): 40-50

Thiam AR, Farese Jr RV, Walther TC (2013) The biophysics and cell biology of lipid droplets. Nat Rev Mol Cell Biol 14: 775-786

Tielrooij KJ, Paparo D, Piatkowski L, Bakker HJ, Bonn M (2009) Dielectric relaxation dynamics of water in model membranes probed terahertz spectroscopy. Biophys J 97 (9): 2484-2492

Tamm LK, Hong H, Liang B (2004) Folding and assembly of β-barrel membrane proteins. Biochim Biophys Acta 166 (1-2): 250-263

Tsumoto K, Ejima D, Senczuk AM, Kita Y, Arakawa T (2007) Effects of salts on protein-surface interactions: applications for column chromatography. J Pharm Sci 96 (7): 1677-1690

Ulmschneider M, Sansom MSP, Nola AD (2006) Evaluating tilt angles of membrane-

associated helices: comparison of computational and NMR techniques. Biophys J 90 (5): 1650-1660

Von Heijne G (2006) Membrane-protein topology. Nat Rev Mol Cell Biol 7: 909-918

Wang E, Erdahl WL, Hamidinia SA, Chapman CJ, Taylor RW, Pfeiffer DR (2001) Transport properties of the calcium ionophore ETH-129. Biophys J 81 (6): 3275-3284

Wilson MA, Pohorille A (1994) Molecular dynamics of a water-lipid bilayer interface. J Am Chem Soc 116 (4): 1490-1501

Wilman HR, Shi J, Deane CM (2014) Helix kinks are equally prevalent in soluble and membrane proteins. Proteins 82 (9): 1960-1970

Xing C, Ollila OHS, Vattulainen, Faller R (2009) Asymmetric nature of lateral pressure profiles in supported lipid membranes and its implications for membrane protein functions. Soft Matter 5 (17): 3258-3261

Xue J, Gao Y, Dong L, Dou J-R, Ma W (2017) Possible effects of electric fields on a pair of spherical cells. J Membr Bio 250 (5): 433-440

Xu Q, Kim M, David Ho KW, Lachowicz P, Fanucci GE, Cafiso DS (2008) Membrane hydrocarbon thickness modulates the dynamics of a membrane transport protein. Biophys J 95 (6): 2849-2858

Yeagle PL (1985) Cholesterol and cell membrane. Biochim Biophys Acta Rev Biomembr 822(3-4): 267-287

Yang Y, Mayer KM, Wickremasinghe NS, Hafner JH (2008) Probing the lipid membrane dipole potential by atomic force microscopy. Biophys J 95 (11): 5193-5199

Zhong M-C, Wei X-B, Zhou J-H, Wang Z-Q, Li Y-M (2013) Trapping red blood cells In living animals using optical tweezers. Nat Commun 4: 1768

Zhou H-X (2010) From induced fit to conformational selection: A continuum of binding mechanism controlled by the timescale of conformational transitions. Biophys J 98 5(6): L15-L17

Zalba S, ten Hagen TLM (2017) Cell membrane modulation as adjuvant in cancer therapy. Cancer Treat Rev 52: 48-57

Zurek N, Sparks L, Voeltz G (2011) Reticulon short hairpin transmembrane domains are used to shape ER tubules. Traffic 12: 28-41

Appendix

Co-author declaration and confirmation

The document is a required enclosure for a compilation of a doctoral thesis at the Department of Natural Sciences, Middlesex University, London

Description of the independent research contributions of the candidate and Co-authors.

Title of the paper: Stretching of red blood cells using an electro-optics trap

Authors: Md Mozzammel Haque, Mihaela G. Moisescu, Sandor Valkai, Andras Der, and Tudor Savopol

The contribution of the candidate:

1. A contribution to the conception and design experiments, performed all of the experiments, development and analysis of a theoretical model, acquisition of data, analysis and interpretation of data.
2. A contribution to drafting the article and revising it critically for important intellectual content.
3. Approval of the version to be published.

Candidate: MD MOZZAMMEL HAQUE

Co-authors' contribution:

1. Mihaela G. Moisescu taught the candidate about the cell culture.
2. Sandor Valkai helped the candidate for simulation using Multiphysics.
3. Tudor Savopol and Mihaela G. Moisescu taught the candidate how to operate optical tweezers.
4. Andras Der who helped the candidate for drafting and revising the article and also an approval of the version for publication.

I have read the declaration from the co-authors and find the descriptions of their contribution in accordance with my view of the cooperation.

Signature of the candidate

Signature of co-author and supervisor